

CERN-EP-2018-092
2018/11/29

CMS-HIG-17-007

Search for the decay of a Higgs boson in the $ll\gamma$ channel in proton-proton collisions at $\sqrt{s} = 13$ TeV

The CMS Collaboration*

Abstract

A search for a Higgs boson decaying into a pair of electrons or muons and a photon is described. Higgs boson decays to a Z boson and a photon ($H \rightarrow Z\gamma \rightarrow ll\gamma, l = e$ or μ), or to two photons, one of which has an internal conversion into a muon pair ($H \rightarrow \gamma^*\gamma \rightarrow \mu\mu\gamma$) were considered. The analysis is performed using a data set recorded by the CMS experiment at the LHC from proton-proton collisions at a center-of-mass energy of 13 TeV, corresponding to an integrated luminosity of 35.9 fb^{-1} . No significant excess above the background prediction has been found. Limits are set on the cross section for a standard model Higgs boson decaying to opposite-sign electron or muon pairs and a photon. The observed limits on cross section times the corresponding branching fractions vary between 1.4 and 4.0 (6.1 and 11.4) times the standard model cross section for $H \rightarrow \gamma^*\gamma \rightarrow \mu\mu\gamma$ ($H \rightarrow Z\gamma \rightarrow ll\gamma$) in the 120–130 GeV mass range of the $ll\gamma$ system. The $H \rightarrow \gamma^*\gamma \rightarrow \mu\mu\gamma$ and $H \rightarrow Z\gamma \rightarrow ll\gamma$ analyses are combined for $m_H = 125$ GeV, obtaining an observed (expected) 95% confidence level upper limit of 3.9 (2.0) times the standard model cross section.

Published in the Journal of High Energy Physics as doi:10.1007/JHEP11(2018)152.

1 Introduction

Measurements of rare decays of the Higgs boson, such as $H \rightarrow \gamma^* \gamma$ and $H \rightarrow Z \gamma$, would enhance our understanding of the standard model (SM) of particle physics, and allow us to probe exotic couplings introduced by possible extensions of the SM [1–4]. The decay width can be modified by the theories involving heavy fermions, gauge bosons or charged scalars [5–9]. Simple extensions of the SM like two Higgs doublet models, or the minimal supersymmetric standard model also exhibit similar features [10]. Certain coefficients of the dimension-6 extension of the standard model effective field theory can be constrained by measuring the $H \rightarrow Z \gamma$ branching ratio precisely [11]. As an example, a model [10] which includes a hypercharge zero triplet extension, shows a modification in $\mathcal{B}(H \rightarrow Z \gamma)$, with respect to the SM value, of about 10% for an additional scalar field with mass between 0 and 400 GeV.

In the search for $H \rightarrow \gamma^* \gamma \rightarrow \ell \ell \gamma$, the leptonic channel, $\gamma^*/Z \rightarrow \ell \ell$ ($\ell = e$ or μ) is most promising as it has relatively low background. The diagrams in Fig. 1 illustrate the dominant Higgs boson decay channels contributing to these final states. The $H \rightarrow \gamma^* \gamma \rightarrow \ell \ell \gamma$ and $H \rightarrow Z \gamma \rightarrow \ell \ell \gamma$ diagrams correspond to the same initial and final state and interfere with each other. Experimentally one can separate the off- and on-shell contributions, and define the respective signal regions, using a selection based on the invariant mass of the dilepton system, $m_{\ell \ell} = m_{\gamma^*/Z}$. For the measurements presented in this paper a threshold of $m_{\ell \ell} = 50$ GeV is used to separate the two processes.

It is informative to express the branching fractions for these decays relative to the $H \rightarrow \gamma \gamma$ process. In the SM, for a Higgs boson with mass $m_H = 125$ GeV [12, 13], these ratios are:

$$\frac{\mathcal{B}(H \rightarrow \gamma^* \gamma \rightarrow \mu \mu \gamma)}{\mathcal{B}(H \rightarrow \gamma \gamma)} = (1.69 \pm 0.10)\%, \quad \frac{\mathcal{B}(H \rightarrow Z \gamma \rightarrow e^+ e^- \gamma / \mu \mu \gamma)}{\mathcal{B}(H \rightarrow \gamma \gamma)} = (2.27 \pm 0.14)\%, \quad (1)$$

where $\mathcal{B}(H \rightarrow Z \gamma \rightarrow e^+ e^- \gamma / \mu \mu \gamma) = 0.051 \times 10^{-3}$ and $\mathcal{B}(H \rightarrow \gamma \gamma) = 2.27 \times 10^{-3}$ are taken from Ref. [14], and $\mathcal{B}(H \rightarrow \gamma^* \gamma \rightarrow \mu \mu \gamma) = 3.83 \times 10^{-5}$ is obtained with the MCFM 7.0.1 program [15], which is in agreement with calculations in Refs. [16–18].

The ATLAS and CMS Collaborations at the CERN LHC have both performed searches for the

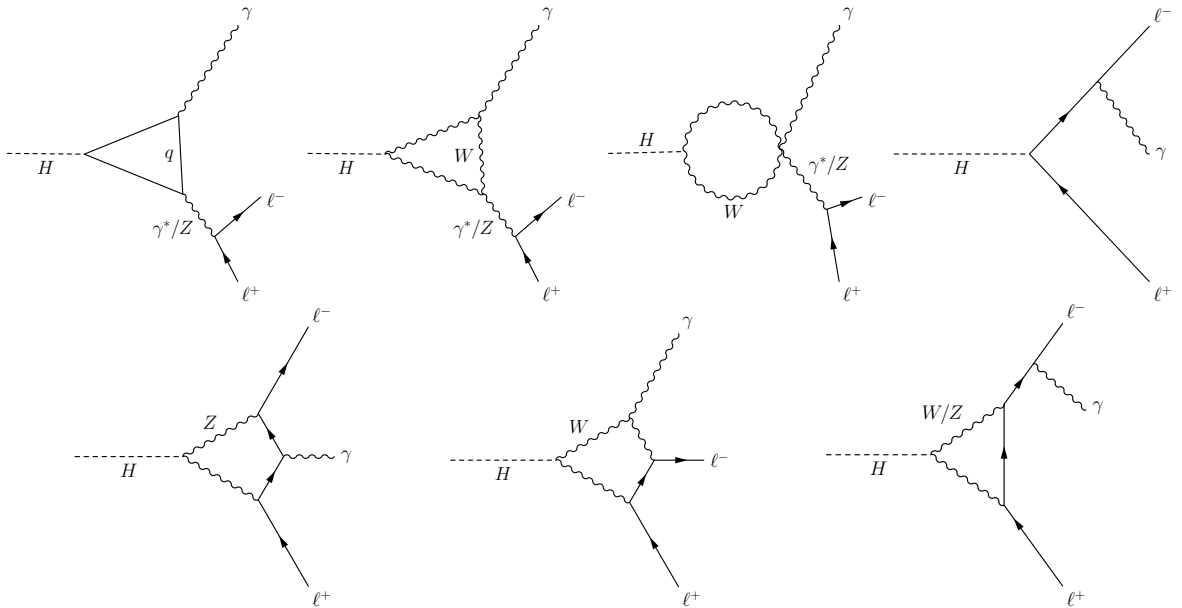


Figure 1: Dominant Feynman diagrams contributing to the $H \rightarrow \ell \ell \gamma$ process.

decay $H \rightarrow Z\gamma \rightarrow \ell\ell\gamma$ [19, 20] at $\sqrt{s} = 7$ and 8 TeV. The ATLAS Collaboration set an upper limit on $\sigma/\sigma_{\text{SM}}$ of 11 (where σ_{SM} is the expected cross section of the SM signal process) at 95% confidence level (CL) for an SM Higgs boson with $m_H = 125.5$ GeV, and the CMS Collaboration set an upper limit of 9.5 at 95% CL for $m_H = 125$ GeV. The CMS Collaboration has also searched for the $H \rightarrow \gamma^*\gamma \rightarrow \ell\ell\gamma$ process with $m_{\ell\ell} < 20$ (1.5) GeV in the dimuon (dielectron) channel at 8 TeV [21]. The two channels were combined to set an upper limit of 6.7 at 95% CL on $\sigma/\sigma_{\text{SM}}$ for $m_H = 125$ GeV. The ATLAS Collaboration has also performed a search for $H \rightarrow Z\gamma \rightarrow \ell\ell\gamma$ at $\sqrt{s} = 13$ TeV using 36.1 fb^{-1} of data collected in 2016. This search set an upper limit on $\sigma/\sigma_{\text{SM}}$ of 6.6 at 95% CL for an SM Higgs boson with $m_H = 125.09$ GeV [22].

This paper describes a search for Higgs bosons decaying to $H \rightarrow \gamma^*\gamma \rightarrow \mu\mu\gamma$ and $H \rightarrow Z\gamma \rightarrow \ell\ell\gamma$ at 13 TeV. The study of the $H \rightarrow \gamma^*\gamma \rightarrow ee\gamma$ decay is challenging [21], because if $m_{\ell\ell}$ is low, the pair of electron showers merge in the electromagnetic calorimeter (ECAL). This merging makes it difficult to trigger on such events and also to reconstruct them offline. Therefore, this channel is not included in the present analysis.

The analysis uses a data sample of proton-proton (pp) collisions at a center-of-mass energy of 13 TeV recorded by the CMS experiment during 2016, corresponding to an integrated luminosity of 35.9 fb^{-1} . The sensitivity of the search is enhanced by dividing the selected events into mutually exclusive classes, according to the expected mass resolution and the signal-to-background ratio, and then combining the results from each class. This paper is structured as follows. In Section 2, the CMS detector is described. The event selection used in the analysis is outlined in Section 3. Section 4 discusses about signal and background modeling. Systematic uncertainties and the results of this study are presented in Section 5, followed by the summary in Section 6.

2 The CMS detector and trigger

A detailed description of the CMS detector can be found in Ref. [23]. The central feature of the CMS apparatus is a superconducting solenoid, 13 m in length and 6 m in diameter, which provides an axial magnetic field of 3.8 T. Within the field volume there are several particle detection systems. Charged-particle trajectories are measured by silicon pixel and silicon strip trackers, covering $0 \leq \phi \leq 2\pi$ in azimuth and $|\eta| < 2.5$ in pseudorapidity. A lead-tungstate crystal ECAL and a brass and scintillator hadron calorimeter (HCAL) surround the tracking volume and cover the region $|\eta| < 3$. They provide energy measurements of photons, electrons and hadronic jets. The ECAL is partitioned into a barrel region with $|\eta| < 1.48$ and two endcaps that extend up to $|\eta| = 3$. A lead and silicon-strip preshower detector is located in front of the endcap of the ECAL. Muons are identified and measured in gas-ionization detectors embedded in the steel return yoke outside the solenoid. The detector is nearly hermetic, allowing energy balance measurements in the plane transverse to the beam direction.

A two-level trigger system selects collision events of interest for physics analysis [24]. The trigger used in the $H \rightarrow \gamma^*\gamma \rightarrow \mu\mu\gamma$ channel requires a muon and a photon with transverse momenta, p_T , greater than 17 and 30 GeV, respectively. The trigger efficiency is determined using signal events in simulation and $\mu\mu\gamma$ events in data using an orthogonal data set selected with a single muon trigger. For events satisfying the selection criteria described in Section 3 the trigger efficiency is 83% in both cases. The $H \rightarrow Z\gamma \rightarrow \ell\ell\gamma$ events are required to pass at least one of the dielectron or dimuon triggers. The dielectron trigger requires a leading (subleading) electron with p_T greater than 23 (12) GeV. The dimuon trigger requires a leading (subleading) muon with p_T greater than 17 (8) GeV. The efficiencies of these dilepton triggers as measured

in data, for events satisfying the selection criteria, are dependent on the p_T and η of the leptons and are measured to be 90–98% and 93–95% for the $ee\gamma$ and $\mu\mu\gamma$ channels, respectively.

3 Event selection

Selected events are required to have at least one good primary vertex, with reconstructed longitudinal position within 24 cm of the geometric center of the detector and transverse position within 2 cm of the beam interaction region. Due to the high instantaneous luminosity of the LHC, there are multiple pp interactions per bunch crossing (pileup). In the case of multiple vertices, the vertex with the largest value of summed physics-object p_T^2 is taken to be the primary pp interaction vertex. The physics objects chosen are those that have been defined using information from the tracking detector, including jets, the associated missing transverse momentum, which is defined as the negative vector sum of the p_T of those jets, and charged leptons. All leptons, which are used to select events, are required to have transverse and longitudinal impact parameters with respect to the primary vertex smaller than 5 and 10 mm, respectively.

The particle-flow (PF) event reconstruction algorithm [25] is used to reconstruct and identify each individual particle using an optimized combination of information from the various elements of the CMS detector.

Photon candidates are reconstructed from clusters of crystals in the ECAL with significant energy deposits [26]. Clusters are grouped into superclusters to recover the energy from electron bremsstrahlung and photons converting in the tracker. In the endcaps, the preshower detector energy is also included for the region covered by the preshower detector ($1.65 < |\eta| < 2.6$). The clustering algorithms result in almost complete recovery of the energy of photons. Photon candidates are selected with a multivariate discriminant that uses, as inputs, isolation variables, the ratio of the energy in the HCAL behind an electromagnetic supercluster to the supercluster energy, and the transverse width of the electromagnetic shower. Isolation variables are based on particle candidates from the PF algorithm. A conversion-safe electron veto [26] is applied to avoid misidentifying an electron as a photon. This vetoes events that have a charged particle track with a hit in the inner layer of the pixel detector that points to the photon cluster in the ECAL, unless that track is matched to a conversion vertex. Photons are required to lie in the geometrical region $|\eta| < 2.5$ and have $p_T > 15$ GeV. The efficiency of the photon identification is measured from $Z \rightarrow ee$ events using tag-and-probe techniques [27]. It is found to be between 84 and 91 (77 and 94)% in the barrel (endcaps) depending on the p_T of the photon, after including the electron veto inefficiencies measured with $Z \rightarrow \mu\mu\gamma$ events, where the photon is produced by final-state radiation.

Electron reconstruction starts from superclusters in the ECAL, which are matched to hits in the silicon strip and the pixel detectors. The energy of electrons is determined from a combination of the electron track momentum at the main interaction vertex and the energy of the corresponding ECAL cluster. Electrons are selected using a multivariate discriminant that includes observables sensitive to the presence of bremsstrahlung along the electron trajectory, the geometrical and momentum-energy matching between the electron trajectory and the energy of the associated cluster in the ECAL, the shape of the electromagnetic shower in the ECAL, and the variables that discriminate against electrons originating from photon conversions [13]. In this analysis, we accept electrons with $p_T > 7$ GeV and $|\eta| < 2.5$.

Muon candidates are reconstructed in the tracker and identified by the PF algorithm using hits in the tracker and the muon systems. The matching between the inner and outer tracks

proceeds either outside-in, starting from a track in the muon system, or inside-out, starting from a track in the silicon tracker. In the latter case, tracks that match track segments in only one or two planes of the muon system are also considered in the analysis in order to collect very low- p_T muons that may not have sufficient energy to penetrate the entire muon system. The muons are selected from the reconstructed muon track candidates by applying minimal requirements on the track in both the muon system and inner tracker system, and taking into account compatibility with small energy deposits in the calorimeters. We accept muons with $p_T > 4 \text{ GeV}$ and $|\eta| < 2.4$ [13].

The relative isolation variable, used to select prompt leptons, is defined as:

$$\mathcal{I}^\ell \equiv \left(\sum p_T^{\text{charged}} + \max [0, \sum p_T^{\text{neutral}} + \sum p_T^\gamma - p_T^{\text{PU}}(\ell)] \right) / p_T^\ell, \quad (2)$$

and is required to be less than 0.35, where $\sum p_T^{\text{charged}}$ is the scalar sum of the transverse momenta of charged hadrons originating from the primary vertex, $\sum p_T^{\text{neutral}}$ and $\sum p_T^\gamma$ are the scalar sums of the transverse momenta for neutral hadrons and photons, respectively, and $\sum p_T^{\text{PU}}(\ell)$ accounts for the contribution of neutral pileup particles. The isolation sums are performed over a cone of angular radius $\Delta R = \sqrt{(\Delta\phi)^2 + (\Delta\eta)^2} = 0.3$ around the lepton direction at the primary vertex. For muons, $p_T^{\text{PU}}(\mu) \equiv 0.5 \sum_i p_T^{\text{PU},i}$, where i runs over the momenta of the charged hadron PF candidates not originating from the primary vertex. For electrons, $p_T^{\text{PU}}(e) \equiv \rho A_{\text{eff}}$, where the effective area A_{eff} is a coefficient that is dependent on electron η and is chosen in such a way that the isolation efficiency is independent of pileup (PU), and ρ is the median of the p_T density distribution for neutral particles [28–30]. Finally, p_T^ℓ is the transverse momentum of the selected lepton. To suppress muons originating from non-prompt decays of hadrons and electrons from photon conversions, we require each lepton track to have a 3D impact parameter with respect to the primary vertex that is less than four times its uncertainty.

The optimized electron selection criteria, including the isolation requirement, give an efficiency of approximately 85–93 (81–92)% in the barrel (endcaps) for electrons from W or Z bosons. For muons, the identification is tuned to maintain efficiency at low ΔR where the two muons are close to each other. The identification and isolation efficiency for single muons from $Z \rightarrow \mu\mu$ or J/ψ meson decays is 85–97 (88–96)% in the barrel (endcaps). In the case of the $H \rightarrow \gamma^* \gamma \rightarrow \mu\mu\gamma$, the $\Delta R(\mu\mu)$ between the two muons is small due to their low invariant mass and the high p_T of the γ^* . Hence, no isolation requirement is applied to the subleading muons as they are within the isolation cone of the leading muons in most events. Also, if the subleading muon falls within the isolation cone of the leading muon, it is not included in the calculation of the isolation variable. The identification efficiency of muons from γ^* is approximately 94–98 (92–97)% in the barrel (endcaps).

Selected events are classified as described in detail below. The dijet-tagged (explained in Section 3.1) event class uses jets that are built by clustering the PF candidates using the anti- k_T clustering algorithm with a distance parameter of 0.4 using the FASTJET software package [28]. Charged PF candidates from pileup vertices are discarded to reduce the contribution to the jet energies from pileup interactions. An offset correction is applied to account for the remaining contributions. In situ measurements of the momentum balance in dijet, photon+jet, Z+jet, and multijet events are used to account for any residual differences in jet energy scale in data and simulation. Additional selection criteria are applied to each event to remove spurious jet-like features originating from isolated noise patterns in certain HCAL regions. Calibrated and corrected jets are required to have p_T greater than 30 GeV and $|\eta| < 4.7$, and to be separated by at least 0.4 in ΔR from leptons and photons passing the selection requirements described above.

3.1 $H \rightarrow \gamma^* \gamma \rightarrow \mu\mu\gamma$ selection

In the $H \rightarrow \gamma^* \gamma \rightarrow \mu\mu\gamma$ search we select events with two muons and a photon, where the muons must have opposite charges and $p_T > 20$ (4) GeV for the leading (subleading) muon. The p_T requirement on the leading muon is driven by the trigger threshold, and that on the subleading muon by the minimum energy needed to reach the muon system. The photon and dimuon transverse momenta both must satisfy $p_T > 0.30m_{\mu\mu\gamma}$, where $m_{\mu\mu\gamma}$ is the invariant mass of the $\mu\mu\gamma$ system. This requirement rejects the γ^* +jet and γ +jet backgrounds without any loss in the signal sensitivity and without introducing a bias in the $m_{\mu\mu\gamma}$ spectrum. The separation between each muon and the photon is required to satisfy $\Delta R > 1$ in order to suppress Drell–Yan background events with final-state radiation.

The dimuon invariant mass is required to be less than 50 GeV to make this selection and the $Z\gamma$ selection described in Section 3.2 mutually exclusive. Events with a dimuon mass in the ranges $2.9 < m_{\mu\mu} < 3.3$ GeV and $9.3 < m_{\mu\mu} < 9.7$ GeV are rejected to avoid $J/\psi \rightarrow \mu\mu$ and $Y(nS) \rightarrow \mu\mu$ contamination, respectively. The invariant mass $m_{\mu\mu\gamma}$ is required to satisfy $110 < m_{\mu\mu\gamma} < 170$ GeV. In the cases where there are multiple dilepton pairs in the event, the one with the smallest dimuon invariant mass is chosen.

A variable R_9 is defined as the energy sum of the 3×3 ECAL crystals centered on the most energetic crystal in the supercluster divided by the energy of the supercluster. The selected events are separated into four mutually exclusive event classes based on the R_9 and η of the photon and the presence of jets. An R_9 value of 0.94 is used to separate the reconstructed photons into two regions. The region containing unconverted photons, with larger values of R_9 and better energy resolution, has a smaller background. By separating events into two regions of low/high R_9 value, the sensitivity of the analysis is increased. We therefore have the following four categories: events that require the presence of at least two jets passing the selection criteria as described below; photon in the ECAL barrel (EB) region with a high R_9 value; photon in the barrel with low R_9 value; and photon in the ECAL endcap (EE) regions. Only events that do not pass the dijet tag are included in the EB or EE classes. By using this event classification scheme, as opposed to combining all events into one class, the sensitivity of this analysis is increased by 11%.

For the dijet tag event class the two highest transverse energy jets are used and the requirements are: (i) the difference in pseudorapidity between the two jets is greater than 3.5; (ii) the Zeppenfeld variable [31] $(\eta_{\ell\ell\gamma} - (\eta_{j1} + \eta_{j2})/2)$ is less than 2.5, where $\eta_{\ell\ell\gamma}$ is the η of the $\ell\ell\gamma$ system and η_{j1} and η_{j2} are the pseudorapidities of the leading and subleading jets, respectively; (iii) the dijet mass is greater than 500 GeV; and (iv) the difference in azimuthal angles between the dijet system and the $\ell\ell\gamma$ system is greater than 2.4. These requirements mainly target the vector boson fusion (VBF) production mechanism of the Higgs boson.

The resulting acceptance times efficiency for $pp \rightarrow H \rightarrow \gamma^* \gamma \rightarrow \mu\mu\gamma$ is 26–27% for m_H between 120 and 130 GeV.

3.2 $H \rightarrow Z\gamma \rightarrow \ell\ell\gamma$ selection

In the $H \rightarrow Z\gamma \rightarrow \ell\ell\gamma$ search, events with a photon and with at least two same-flavor leptons (e or μ) consistent with a Z boson decay are selected. All particles must be isolated, and have p_T greater than 25 (15) GeV for the leading (subleading) electron, 20 (10) GeV for the leading (subleading) muon, and 15 GeV for the photon. In the cases where there are multiple dilepton pairs in the event, the one with the mass closest to the Z boson nominal mass [32] is selected. The invariant mass of the selected pair is required to be larger than 50 GeV. This

ensures that the $H \rightarrow Z\gamma \rightarrow \ell\ell\gamma$ event selection is orthogonal to that for $H \rightarrow \gamma^*\gamma \rightarrow \mu\mu\gamma$.

The events are required to have a photon with $E_T > 0.14m_{\ell\ell\gamma}$, which rejects the Z+jets background without significant loss in signal sensitivity and without introducing a bias in the $m_{\ell\ell\gamma}$ spectrum. Leptons are required to have $\Delta R > 0.4$ with respect to the photon in order to reject events with final-state radiation. In addition, we require $m_{\ell\ell\gamma} + m_{\ell\ell} > 185$ GeV to reject events with final-state radiation from Drell–Yan processes. Finally, the invariant mass of the $\ell\ell\gamma$ system is required to be $115 < m_{\ell\ell\gamma} < 170$ GeV.

The selected events are classified into mutually exclusive categories. A lepton-tag class contains events with an additional electron (or muon) with $p_T > 7$ (5) GeV, to target Higgs boson production in association with either a Z or W boson. Events not included in the lepton class are considered for the dijet class. In this case the criteria described in Section 3.1 are used to select events containing a dijet, targeting Higgs boson production in a VBF process. The next class considered is the boosted class, which requires that the p_T of the $\ell\ell\gamma$ system is greater than 60 GeV in order to enhance the fraction of events that contain a Lorentz-boosted Higgs boson recoiling against a jet. Events that do not fall into these three classes are placed in the untagged categories. A significant fraction of the signal events are expected to have the photon and both leptons in the barrel, while only a sixth of the signal events have the photon in the endcap. This is in contrast to the background, where about one third of the events are expected to have a photon in the endcap. Furthermore, events where the photon does not convert to e^+e^- have a smaller fraction of background events and better energy resolution. For these reasons, the untagged events are classified into four categories according to the pseudorapidity of the leptons and photon, and the R_9 value of the photon. These categories are indicated as untagged 1, untagged 2, untagged 3 and untagged 4 as shown in Table 1.

It should be noted that the electron and muon channels are considered separately in all classes except for the lepton-tag class where the number of events is small. This event classification scheme increases the sensitivity of the analysis by 18%. The resulting acceptance times efficiency for $pp \rightarrow H \rightarrow Z\gamma \rightarrow \ell\ell\gamma$ in the electron (muon) channel is between 18 and 24 (25 and 31)% for m_H between 120 and 130 GeV.

A complete list of all the categories considered in the analysis ($pp \rightarrow H \rightarrow \gamma^*\gamma \rightarrow \mu\mu\gamma$ and $pp \rightarrow H \rightarrow Z\gamma \rightarrow \ell\ell\gamma$), together with the expected yields for a 125 GeV SM Higgs boson signal processes, is shown in Table 2. This table also reports yields from signal processes: gluon-gluon fusion (ggH), vector boson fusion (VBF), associated VH production (VH) and Higgs boson production in association with top quarks ($t\bar{t}H$).

4 Signal and background modeling

The search for signal events is performed using a shape-based analysis of $\ell\ell\gamma$ invariant mass distributions. The background is estimated from data and the signal is estimated using the simulation. Even though the background is estimated from data, simulated samples are used in the $H \rightarrow Z\gamma \rightarrow \ell\ell\gamma$ search to optimize the event classes. The main background, $pp \rightarrow Z\gamma$, is generated at next-to-leading order (NLO) using the MADGRAPH5_aMC@NLO generator [33]. The $Z(\ell\ell)$ +jets events with a jet misidentified as a photon are another important source of background and are generated at NLO using MADGRAPH5_aMC@NLO. The NLO parton distribution function (PDF) set, NNPDF3.0 [34], and the CUETP8M1 [35] underlying event tune are used to generate these samples. All background events are interfaced with PYTHIA 8.205 [36, 37] for the fragmentation and hadronization of partons.

Table 1: Categories in $H \rightarrow Z\gamma \rightarrow \ell\ell\gamma$ search. The electron and muon channels are considered separately in all classes except for the lepton-tag class.

| Category | $e^+e^-\gamma$ | $\mu^+\mu^-\gamma$ |
|------------|--|--|
| Lepton tag | Additional electron ($p_T > 7$ GeV) or muon ($p_T > 5$ GeV) | |
| Dijet tag | At least 2 jets required dijet selection (Section 3.1) | At least 2 jets required dijet selection (Section 3.1) |
| Boosted | $p_T(ee\gamma) > 60$ GeV | $p_T(\mu\mu\gamma) > 60$ GeV |
| Untagged 1 | Photon $0 < \eta < 1.4442$ Both leptons $0 < \eta < 1.4442$ $R_9 > 0.94$ | Photon $0 < \eta < 1.4442$ Both leptons $0 < \eta < 2.1$ and one lepton $0 < \eta < 0.9$ $R_9 > 0.94$ |
| Untagged 2 | Photon $0 < \eta < 1.4442$ Both leptons $0 < \eta < 1.4442$ $R_9 < 0.94$ | Photon $0 < \eta < 1.4442$ Both leptons $0 < \eta < 2.1$ and one lepton $0 < \eta < 0.9$ $R_9 < 0.94$ |
| Untagged 3 | Photon $0 < \eta < 1.4442$ At least one lepton $1.4442 < \eta < 2.5$ No requirement on R_9 | Photon $0 < \eta < 1.4442$ Both leptons in $ \eta > 0.9$ or one lepton in $2.1 < \eta < 2.4$ No requirement on R_9 |
| Untagged 4 | Photon $1.566 < \eta < 2.5$ Both leptons $0 < \eta < 2.5$ No requirement on R_9 | Photon $1.566 < \eta < 2.5$ Both leptons $0 < \eta < 2.4$ No requirement on R_9 |

Signal samples for the $H \rightarrow \gamma^*\gamma \rightarrow \mu\mu\gamma$ produced via ggH, VBF, and VH processes are simulated at NLO with MADGRAPH5_aMC@NLO 2.3.3, with the Higgs boson characterization framework [38, 39]. The ttH production mechanism gives a negligible contribution to the signal and is therefore ignored. For the $H \rightarrow Z\gamma \rightarrow \ell\ell\gamma$ process, the simulated events from all four production mechanisms are generated at NLO using POWHEG v2.0 [40, 41]. All signal samples are interfaced with PYTHIA 8.212 with the CUETP8M1 underlying event tune for hadronization and fragmentation. The NLO PDF set, NNPDF3.0, is used to produce these samples. The SM Higgs boson production cross sections and branching fractions recommended by the LHC Higgs cross section working group [14] are used for $H \rightarrow Z\gamma$, whereas for $H \rightarrow \gamma^*\gamma$ the Higgs boson production cross sections are also taken from Ref. [14], but the branching fraction of $H \rightarrow \gamma^*\gamma$ is taken from the MCFM calculation and given in Eq.(1).

The simulated signal and background events are reweighted by taking into account the difference between data and simulated events so that the distribution of pileup vertices, the trigger efficiencies, the resolution, the energy scale, the reconstruction efficiencies, and the isolation efficiency—for electrons, muons, and photons—observed in data are reproduced. An additional correction is applied to photons to reproduce the performance of the R_9 shower shape variable.

The dominant backgrounds to $H \rightarrow \ell\ell\gamma$ consist of the irreducible non-resonant SM $\ell\ell\gamma$ production, final-state radiation in Z decays, γ^* conversions, and Drell–Yan production in association

Table 2: Expected signal yields for a 125 GeV SM Higgs boson, corresponding to an integrated luminosity of 35.9 fb^{-1} , for all categories in the $H \rightarrow \gamma^* \gamma \rightarrow \mu\mu\gamma$ and $H \rightarrow Z\gamma \rightarrow \ell\ell\gamma$ processes in the narrowest $\ell\ell\gamma$ invariant mass window around 125 GeV containing 68.3% of the expected signal distribution.

| Analysis | Channel | Category | Number of signal events for $m_H = 125 \text{ GeV}$ | | |
|--|---------------|----------------|--|-------|----------|
| | | | ggH | VBF | VH + ttH |
| $H \rightarrow \gamma^* \gamma \rightarrow \mu\mu\gamma$ | $\mu\mu$ | EB, high R_9 | 9.18 | 0.47 | 0.33 |
| | $\mu\mu$ | EB, low R_9 | 5.17 | 0.27 | 0.18 |
| | $\mu\mu$ | EE | 3.80 | 0.20 | 0.25 |
| | $\mu\mu$ | Dijet tag | 0.45 | 0.39 | 0.01 |
| $H \rightarrow Z\gamma \rightarrow \ell\ell\gamma$ | $ee + \mu\mu$ | Lepton tag | 0.08 | 0.014 | 0.33 |
| | ee | Dijet tag | 0.34 | 0.47 | 0.02 |
| | ee | Boosted | 3.38 | 0.56 | 0.33 |
| | ee | Untagged 1 | 5.2 | 0.15 | 0.06 |
| | ee | Untagged 2 | 3.2 | 0.09 | 0.04 |
| | ee | Untagged 3 | 3.9 | 0.12 | 0.06 |
| | ee | Untagged 4 | 2.8 | 0.08 | 0.04 |
| | $\mu\mu$ | Dijet tag | 0.44 | 0.62 | 0.02 |
| | $\mu\mu$ | Boosted | 4.51 | 0.74 | 0.44 |
| | $\mu\mu$ | Untagged 1 | 7.6 | 0.22 | 0.097 |
| | $\mu\mu$ | Untagged 2 | 4.8 | 0.14 | 0.06 |
| | $\mu\mu$ | Untagged 3 | 4.1 | 0.12 | 0.06 |
| | $\mu\mu$ | Untagged 4 | 3.5 | 0.11 | 0.06 |

with jets, where a jet or a lepton is misidentified as a photon.

The background is estimated from data, by fitting the observed $\ell\ell\gamma$ mass distributions. Separate fits are performed to the four event classes for the $H \rightarrow \gamma^* \gamma \rightarrow \mu\mu\gamma$ analysis and the thirteen classes for the $H \rightarrow Z\gamma \rightarrow \ell\ell\gamma$ analysis. For the $H \rightarrow \gamma^* \gamma \rightarrow \mu\mu\gamma$ ($H \rightarrow Z\gamma \rightarrow \ell\ell\gamma$) analysis, the range $110(115) < m_{\ell\ell\gamma} < 170 \text{ GeV}$ is used in the fit. The fit model of the signal is obtained from an unbinned fit to the mass distribution of the corresponding sample of simulated events, using a double Crystal Ball function [42] in the $H \rightarrow \gamma^* \gamma \rightarrow \mu\mu\gamma$ analysis, and a Crystal Ball function plus a Gaussian function in the $H \rightarrow Z\gamma \rightarrow \ell\ell\gamma$ analysis. To derive the signal shapes for the intermediate mass points where simulation was not available, a linear interpolation of the fitted parameters for available mass points was performed.

The choice of the background fit function is based on a study that minimizes the bias that could be introduced by the selected function. The study of the bias is performed for four families of functions:

1. A sum of N exponential functions

$$\sum_{i=1}^N f_i e^{p_i m_{\ell\ell\gamma}} \quad (3)$$

with $2N$ free parameters: $p_i < 0$ and f_i . The lowest order considered has $N = 1$.

2. A sum of N power-functions

$$\sum_{i=1}^N f_i m_{\ell\ell\gamma}^{p_i} \quad (4)$$

with $2N$ free parameters $p_i < 0$ and f_i . The lowest order considered has $N = 1$.

3. Bernstein polynomials of N th order, with $N = 1, 2, 3, 4,$ and 5

$$\text{Ber}_N(m_{\ell\ell\gamma}) = \sum_{i=1}^N f_i^2 \binom{N}{i} m_{\ell\ell\gamma}^i (1 - m_{\ell\ell\gamma})^{N-i} \quad (5)$$

with N free parameters f_i .

4. Laurent series with $N = 2, 3,$ and 4 terms

$$f_2 m_{\ell\ell\gamma}^{-4} + f_3 m_{\ell\ell\gamma}^{-5} \quad (6)$$

$$f_1 m_{\ell\ell\gamma}^{-3} + f_2 m_{\ell\ell\gamma}^{-4} + f_3 m_{\ell\ell\gamma}^{-5} \quad (7)$$

and

$$f_1 m_{\ell\ell\gamma}^{-3} + f_2 m_{\ell\ell\gamma}^{-4} + f_3 m_{\ell\ell\gamma}^{-5} + f_4 m_{\ell\ell\gamma}^{-6} \quad (8)$$

with N free parameters $f_{1\dots N}$.

A test is then performed to determine the best order in each family. This test uses the difference in the negative log-likelihood (NLL) between the fits performed to data with two different orders of the same family of functions. The test starts with the lowest order N in that family of functions and the order is increased to the $(N+M)^{th}$ order until the data support the hypothesis of the higher-order function. For this purpose, a p -value of this quantity is calculated as:

$$p\text{-value} = \text{Prob}(2\Delta NLL > 2\Delta NLL_{N+M} | \chi^2(M)), \quad (9)$$

where ΔNLL is the difference of log-likelihood between the two fits; $\Delta NLL_{N+M} = 2(NLL_N - NLL_{N+M})$ follows a χ^2 distribution with M degrees of freedom, where M is the difference in the number of free parameters between the $N+M$ function and the N function; NLL_N and NLL_{N+M} are the values of the log-likelihood of the fit to data using N^{th} and $(N+M)^{th}$ order functions from a family. If the p -value is less than 0.05, the higher order function is supported by the data and the procedure is then applied to other higher order functions in the same family. The procedure stops when the p -value becomes greater than 0.05.

Once the best order of each family is determined for each category, pseudo-experiments (with no injected signal) describing possible experimental outcomes are randomly generated using each of the determined functions as generators of background. A signal-plus-background fit is performed for each of these sets of pseudo-experiments with all other background functions of the chosen order, so that the presence of a possible bias introduced by the fitting function can be determined. In each fit, the bias is estimated with a pull variable, computed as $(\mu_{\text{FIT}} - \mu_t) / \sigma_{\text{FIT}}$, where μ_{FIT} and σ_{FIT} are the mean and the standard deviation of the signal strength determined from the signal-plus-background fit, and μ_t is the true injected signal strength, which is zero in this case. A given fit function is deemed acceptable in a given category if its pull is less than 0.14 when fitting pseudo-experiments generated with all of the other functional families. With this requirement, the error on the frequentist coverage of the quoted measurement in the analysis is less than 1%, where the coverage is defined as the fraction of experiments in which the true

Table 3: Fit functions chosen as a result of the bias study used in the analysis.

| $m_{\ell\ell}$ | Category | Best fit function |
|----------------|----------------|------------------------|
| <50 GeV | EB, high R_9 | Bernstein of order 4 |
| | EB, low R_9 | Bernstein of order 4 |
| | EE | Bernstein of order 4 |
| | Dijet tag | Exponential of order 2 |
| >50 GeV | Lepton tag | Power law of order 1 |
| | Dijet tag | Power law of order 1 |
| | Boosted | Bernstein of order 3 |
| | Untagged 1 | Bernstein of order 4 |
| | Untagged 2 | Bernstein of order 5 |
| | Untagged 3 | Bernstein of order 4 |
| | Untagged 4 | Bernstein of order 4 |

value is contained within the confidence interval. If several functions pass this criterion, then we choose the one which has the least pull. Table 3 shows the fit functions chosen in each category of the analysis.

The background fits based on the $m_{\ell\ell\gamma}$ data distributions for the event categories of the $H \rightarrow \gamma^*\gamma \rightarrow \mu\mu\gamma$ analysis are shown in Fig. 2 and, for the electron and muon channels in all $H \rightarrow Z\gamma \rightarrow \ell\ell\gamma$ event class definitions except for the lepton tag category, in Figs. 3 and 4 respectively. Finally, Fig. 5 shows the background fit for the lepton tag category in the $H \rightarrow Z\gamma \rightarrow \ell\ell\gamma$ analysis. As we can see from these figures, the background fits describe the data well.

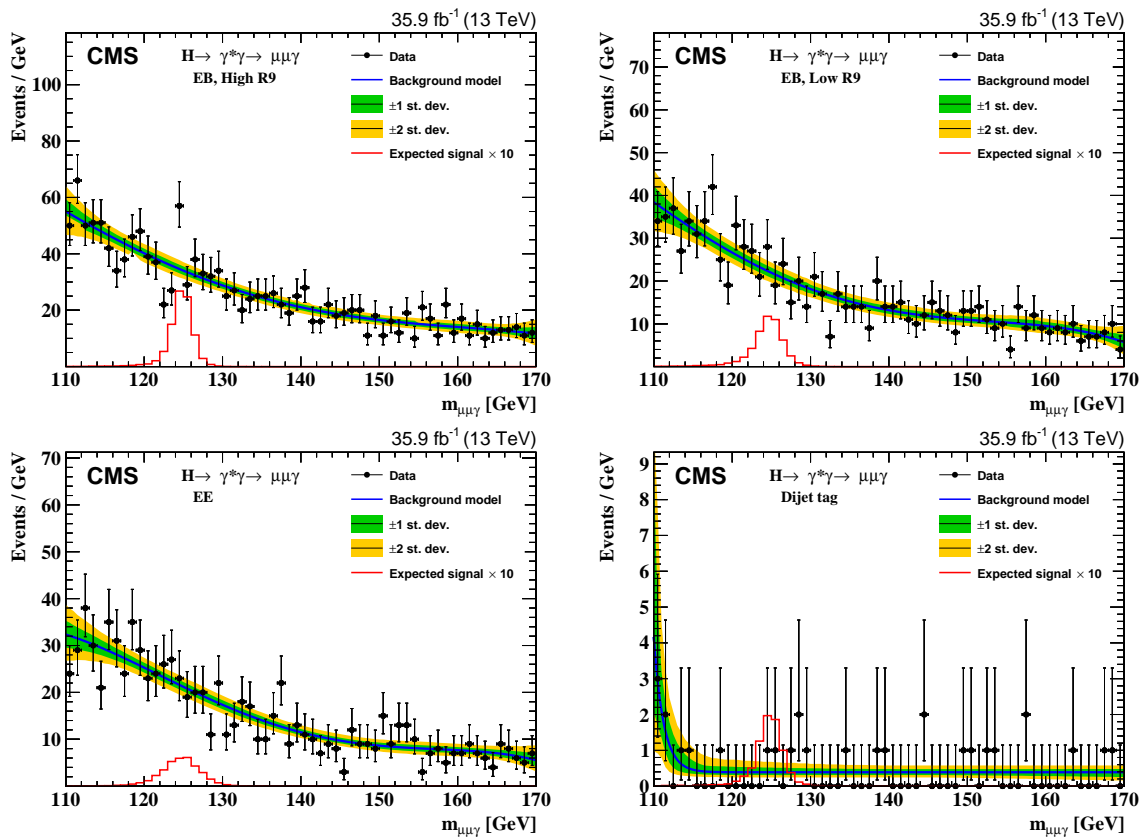


Figure 2: Background model fit to the $m_{\mu\mu\gamma}$ distribution for EB-high R_9 (upper left), EB-low R_9 (upper right), EE (lower left) and dijet tag (lower right) for the $H \rightarrow \gamma^*\gamma \rightarrow \mu\mu\gamma$ selection. The green and yellow bands represent the 68 and 95% CL uncertainties in the fit to the data.

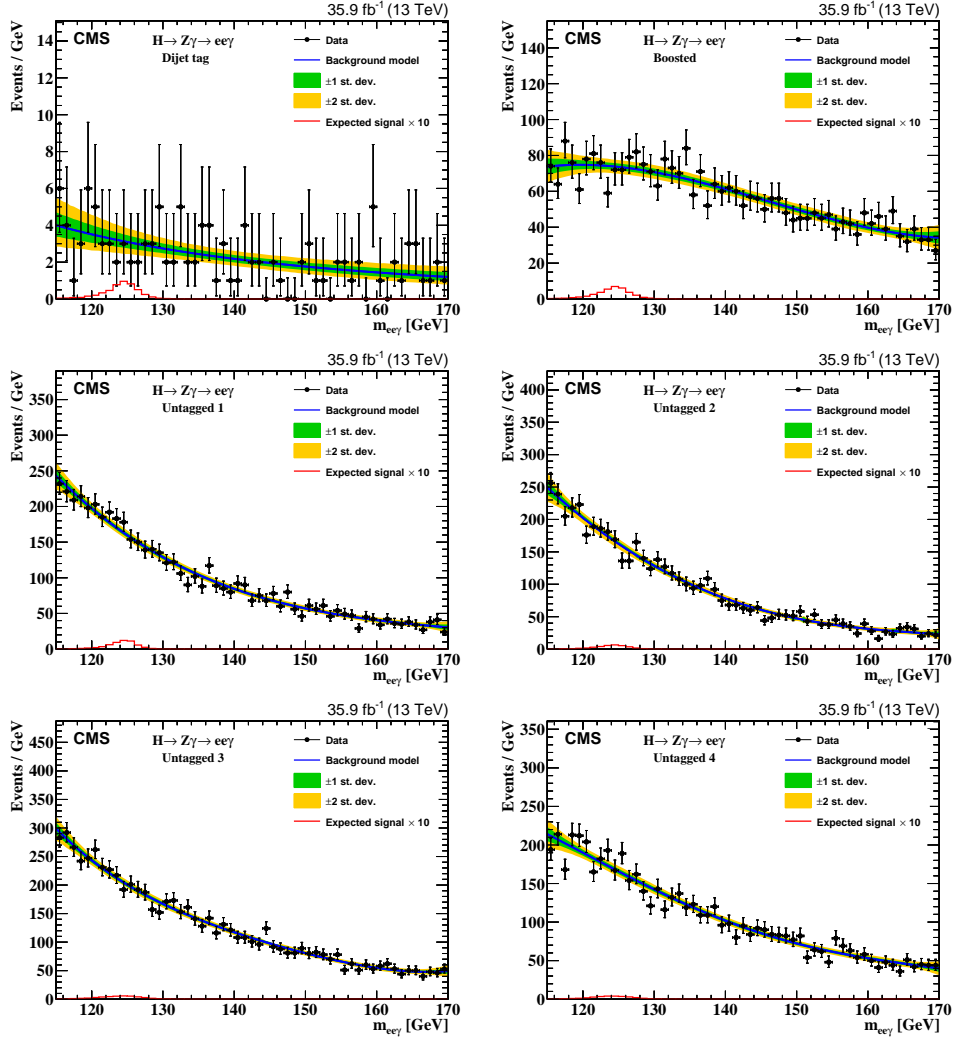


Figure 3: Background model fit to the $m_{ee\gamma}$ distribution for dijet tag (upper left), boosted (upper right), untagged 1 (middle left), untagged 2 (middle right), untagged 3 (bottom left), and untagged 4 (bottom right) for the $H \rightarrow Z\gamma \rightarrow ee\gamma$ selection. The green and yellow bands represent the 68 and 95% CL uncertainties in the fit to the data.

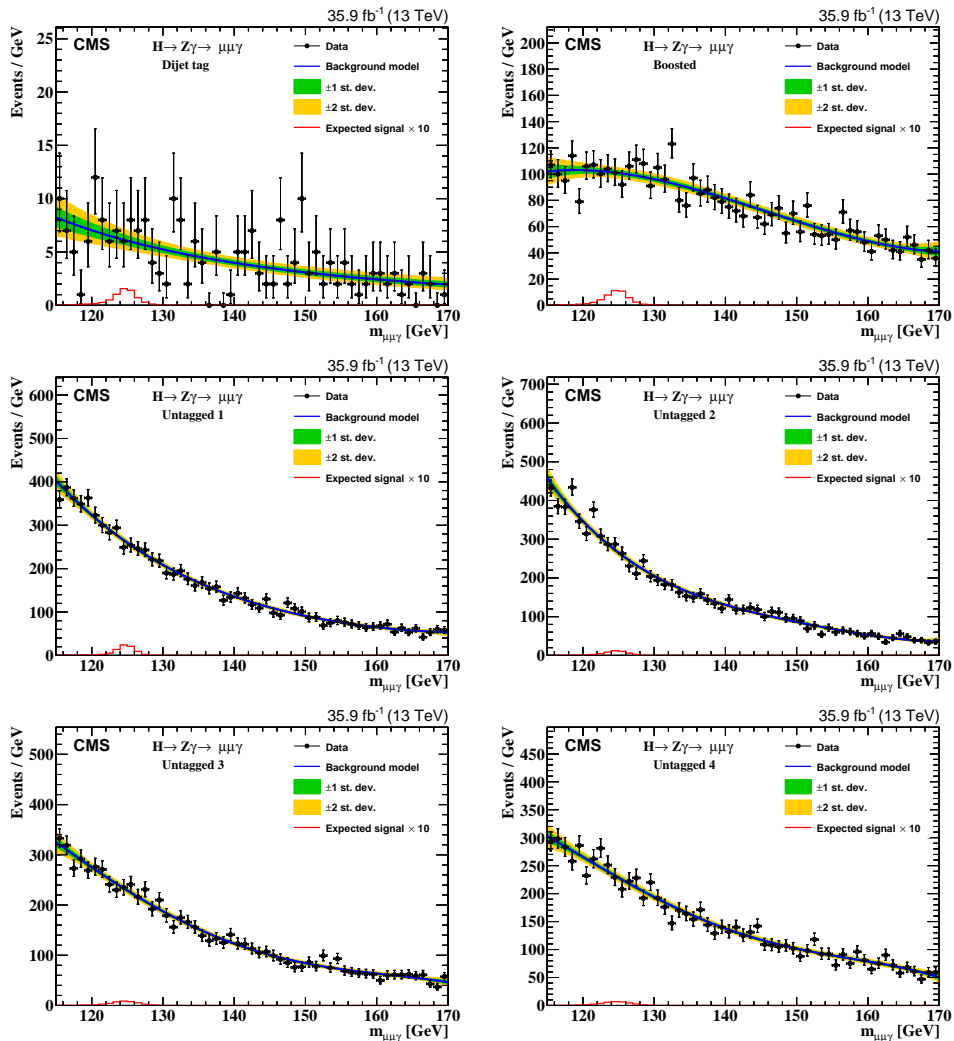


Figure 4: Background model fit to the $m_{\mu\mu\gamma}$ distribution for dijet tag (upper left), boosted (upper right), untagged 1 (middle left), untagged 2 (middle right), untagged 3 (bottom left), and untagged 4 (bottom right) for the $H \rightarrow Z\gamma \rightarrow \mu\mu\gamma$ selection. The green and yellow bands represent the 68 and 95% CL uncertainties in the fit to the data.

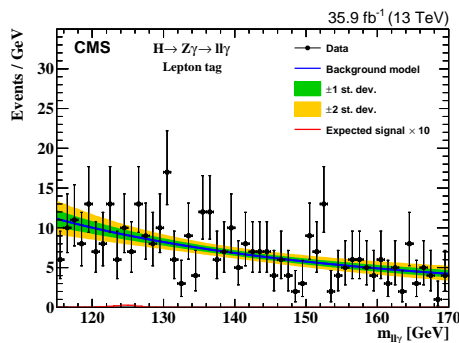


Figure 5: Background model fit to the $m_{\ell\ell\gamma}$ distribution for $H \rightarrow Z\gamma \rightarrow \ell\ell\gamma$ lepton tag category. The green and yellow bands represent the 68 and 95% CL uncertainties in the fit to the data.

5 Systematic uncertainties and results

No significant deviation from the background-only hypothesis is observed. The data are used to derive upper limits on the Higgs boson production cross section times the branching fractions, $\sigma(\text{pp} \rightarrow \text{H}) \mathcal{B}(\text{H} \rightarrow \gamma^* \gamma \rightarrow \mu\mu\gamma)$ and $\sigma(\text{pp} \rightarrow \text{H}) \mathcal{B}(\text{H} \rightarrow Z\gamma \rightarrow \ell\ell\gamma)$, divided by the corresponding SM predictions. The limits are evaluated using a modified frequentist approach, asymptotic CL_s , taking the profile likelihood as a test statistic [43–46]. An unbinned evaluation of the likelihood is considered.

Background uncertainties are taken from the fit to the data. The sources of systematic uncertainties related to the signal are listed below. The first two sources affect the signal shape and the remaining sources affect the signal yield.

- Electron and photon energy scale and resolution: The electromagnetic energy scale is known with 0.15–0.5 (1)% precision in EB (EE). To quantify the corresponding uncertainty, the electron and photon energies are varied and the effects on signal mean and resolution are propagated as shape nuisance parameters in the estimation of limits.
- Muon momentum scale and resolution: The uncertainty in the muon momentum scale is 1%. To quantify the corresponding uncertainty, the muon momentum scale is varied and the effect on signal mean and resolution is propagated as a shape nuisance parameter in the estimation of limits.
- Integrated luminosity: The uncertainty in the integrated luminosity is 2.5% [47]. This is applied as a normalization uncertainty to the total expected yield of the signal.
- Object identification and isolation: The corrections applied to the simulation to reproduce the performance of the lepton and photon selection are measured with $Z \rightarrow ee$ and $Z \rightarrow \mu\mu$ events.
- Pileup: The uncertainty from the description of the pileup in the signal simulation is estimated by varying the total inelastic cross section by $\pm 4.6\%$ [48].
- Jet-energy scale and resolution: The uncertainties in the jet energy scale and resolution are accounted for by changing the jet response and resolution by $\sim 2\%$.
- Underlying event and parton shower uncertainty: The uncertainty associated with the choice and tuning of the generator is estimated with dedicated samples which are generated by varying the parameters of the tune used (CUETP8M1) to generate the original signal samples. The difference in signal yields with respect to the nominal configuration is propagated as the uncertainty.
- R_9 reweighting: This shower-shape variable in the signal simulation is reweighted to match that in the data. This reweighting introduces an uncertainty that is estimated by removing the R_9 reweighting in the simulation and then estimating the yields in the categories where R_9 is used for categorization.
- Theoretical uncertainties: These include the systematic uncertainties from the effect of the choice of PDF on the signal cross section [49–51] and the uncertainty in the Higgs boson branching fraction prediction. The uncertainty in the branching ratio of $\text{H} \rightarrow Z\gamma$ is calculated to be 5.6% [14]. In the case of $\text{H} \rightarrow \gamma^* \gamma$ analysis, there is no available theoretical uncertainty. So it is taken by rounding off the error on the branching ratio of $\text{H} \rightarrow Z\gamma$ to 6%.

The pre-fit values of the nuisance parameters, averaged over all the categories, are summarized

in Table 4.

Table 4: Sources of systematic uncertainties considered in the $H \rightarrow Z\gamma \rightarrow \ell\ell\gamma$ and $H \rightarrow \gamma^*\gamma \rightarrow \mu\mu\gamma$ analyses. The pre-fit values of the nuisance parameters are shown averaged over all the categories in the analysis which either affect the normalization of the simulated signal event yields or the mean and resolution of $m_{\ell\ell\gamma}$. The “—” indicates that the uncertainty is not applicable.

| Sources | $H \rightarrow Z\gamma \rightarrow \ell\ell\gamma$ | $H \rightarrow \gamma^*\gamma \rightarrow \mu\mu\gamma$ |
|-------------------------------------|--|---|
| Theory | | |
| – ggH cross section (scale) | 3.9% | 3.9% |
| – ggH cross section (PDF) | 3.2% | 3.2% |
| – VBF cross section (scale) | +0.4% – 0.3% | +0.4% – 0.3% |
| – VBF cross section (PDF) | 2.1% | 2.1% |
| – WH cross section (scale) | +0.5% – 0.7% | +0.5% – 0.7% |
| – WH cross section (PDF) | 1.9% | 1.9% |
| – ZH cross section (scale) | +3.8% – 3.1% | +3.8% – 3.1% |
| – ZH cross section (PDF) | 1.6% | 1.6% |
| – ttH cross section (scale) | +5.8% – 9.2% | — |
| – ttH cross section (PDF) | 3.6% | — |
| Underlying event and parton shower | | |
| – Muon channel | 3% | 4.7% |
| – Electron channel | 3% | — |
| Branching fraction | 5.7% | 6% |
| Integrated luminosity | 2.5% | 2.5% |
| Lepton identification and isolation | | |
| – Muon channel | 0.6% | 2% |
| – Electron channel | 1.2% | — |
| Photon identification and isolation | | |
| – Muon channel | 2.3% | 1.6% |
| – Electron channel | 2.2% | — |
| Pileup reweighting | | |
| – Muon channel | 0.6% | 0.3% |
| – Electron channel | 0.9% | — |
| R_9 reweighting | | |
| – Muon channel | 6.5% | 9% |
| – Electron channel | 6.8% | — |
| Trigger | | |
| – Muon channel | 1.3% | 4% |
| – Electron channel | 1% | — |
| Energy and momentum (muon channel) | | |
| – Signal mean | 0.04% | 0.08% |
| – Signal resolution | 4% | 5% |
| Energy (electron channel) | | |
| – Signal mean | 0.15% | — |
| – Signal resolution | 4% | — |
| Jet energy scale | | |
| – Muon channel | 2.5% | 3.8% |
| – Electron channel | 2.7% | — |
| Jet energy resolution | | |
| – Muon channel | 0.3% | 0.7% |
| – Electron channel | 0.3% | — |

Based on the fit bias studies, the uncertainty in the background estimation due to the chosen functional form is assumed to be negligible. Furthermore, to combine the $H \rightarrow Z\gamma \rightarrow \ell\ell\gamma$ and $H \rightarrow \gamma^*\gamma \rightarrow \mu\mu\gamma$ channels, uncertainties from theoretical sources, integrated luminosity,

object identification, R_9 reweighting, jet energy correction and resolution are considered to be correlated across the categories.

The expected and observed exclusion limits at 95% CL for the process $H \rightarrow \gamma^* \gamma \rightarrow \mu\mu\gamma$ are shown in Fig 6. The expected limits are between 2.1 and 2.3 times the SM cross section and the observed limit varies between about 1.4 and 4.0 times the SM cross section. The limits are calculated at 1 GeV intervals in the mass range of $120 < m_H < 130$ GeV. Figure 6 also shows the combined limit for the $H \rightarrow Z\gamma \rightarrow \ell\ell\gamma$ channel. The expected exclusion limits at 95% CL are between 3.9 and 9.1 times the SM cross section and the observed limit varies between about 6.1 and 11.4 times the SM cross section.

Finally, Fig. 7 shows the expected limit for each category and the combined limit for both channels for $m_H = 125$ GeV. The combined observed (background only expected) limit is 3.9 (2.0) for a 125 GeV Higgs boson decaying to $\ell\ell\gamma$. The same figure shows the combined expected limit of 2.9, assuming an SM Higgs boson with $m_H = 125$ GeV, decaying to the $\ell\ell\gamma$ channel. After combining both analyses, $H \rightarrow \gamma^* \gamma \rightarrow \mu\mu\gamma$ and $H \rightarrow Z\gamma \rightarrow \ell\ell\gamma$ and considering the background-only hypothesis, the observed p -value at $m_H = 125$ GeV is 0.02, which corresponds to about two standard deviations. The combined expected p -value for an SM Higgs boson at $m_H = 125$ GeV is 0.16, corresponding to a significance of around one standard deviation.

6 Summary

A search is performed for a standard model (SM) Higgs boson decaying into a lepton pair and a photon. This final state has contributions from Higgs boson decays to a Z boson and a photon ($H \rightarrow Z\gamma \rightarrow \ell\ell\gamma, \ell = e$ or μ), or to two photons, one of which has an internal conversion into a muon pair ($H \rightarrow \gamma^* \gamma \rightarrow \mu\mu\gamma$). The analysis is performed using a data set from pp collisions at a center-of-mass energy of 13 TeV, corresponding to an integrated luminosity of 35.9 fb^{-1} . No significant excess above the expected background is found. Limits on the Higgs boson production cross section times the corresponding branching fractions are set. The expected exclusion limits at 95% confidence level are about 2.1–2.3 (3.9–9.1) times the SM cross section in the $H \rightarrow \gamma^* \gamma \rightarrow \mu\mu\gamma$ ($H \rightarrow Z\gamma \rightarrow \ell\ell\gamma$) channel in the mass range from 120 to 130 GeV, and the observed limit varies between about 1.4 and 4.0 (6.1 and 11.4) times the SM cross section. Finally, the $H \rightarrow \gamma^* \gamma \rightarrow \mu\mu\gamma$ and $H \rightarrow Z\gamma \rightarrow \ell\ell\gamma$ analyses are combined for $m_H = 125$ GeV, obtaining an observed (expected) 95% confidence level upper limit of 3.9 (2.0) times the SM cross section.

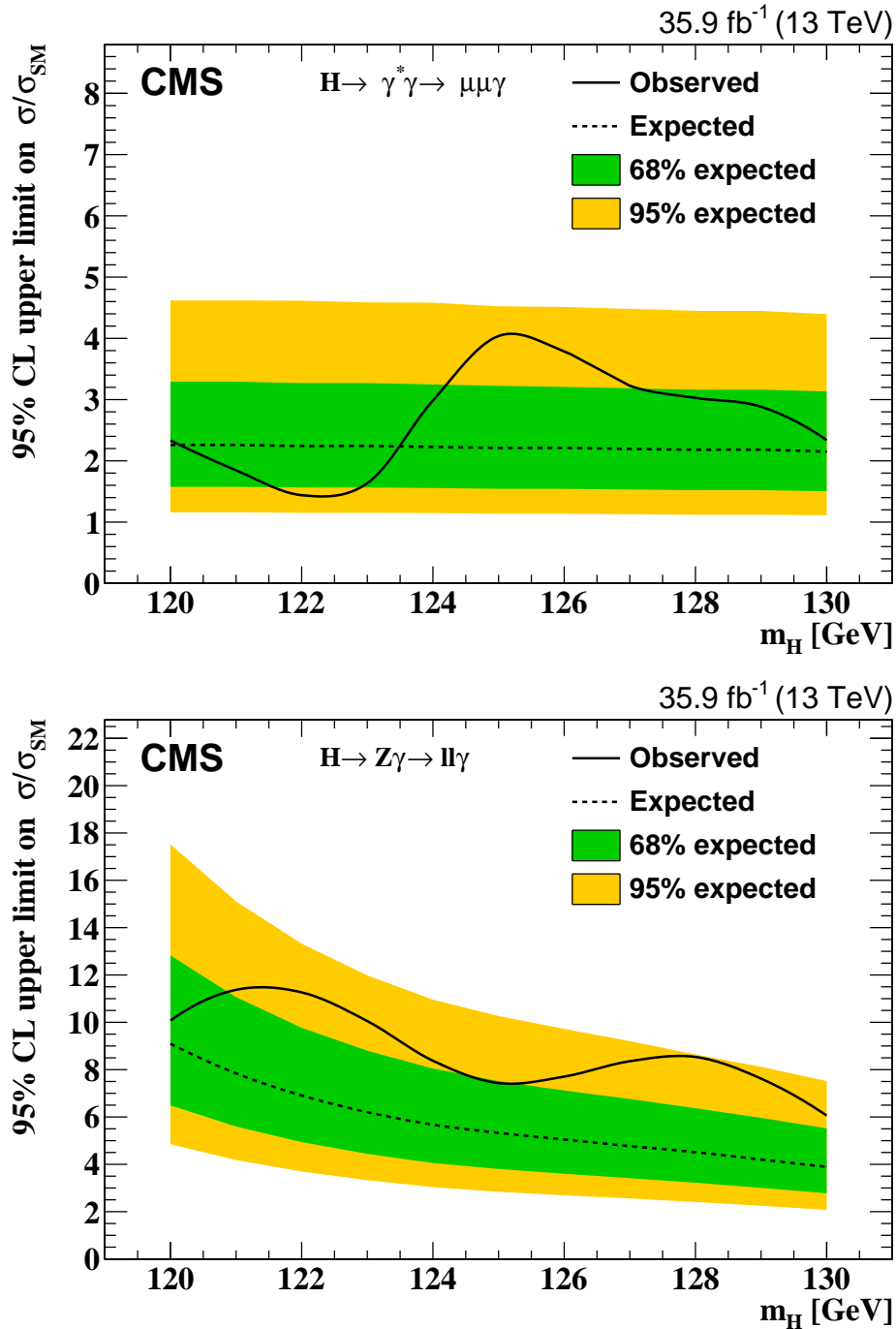


Figure 6: Exclusion limit, at 95% CL, on the cross section of the $\text{H} \rightarrow \gamma^* \gamma \rightarrow \mu\mu\gamma$ process (upper plot) and the $\text{H} \rightarrow \text{Z}\gamma \rightarrow \ell\ell\gamma$ process (lower plot) relative to the SM prediction, as a function of the Higgs boson mass.

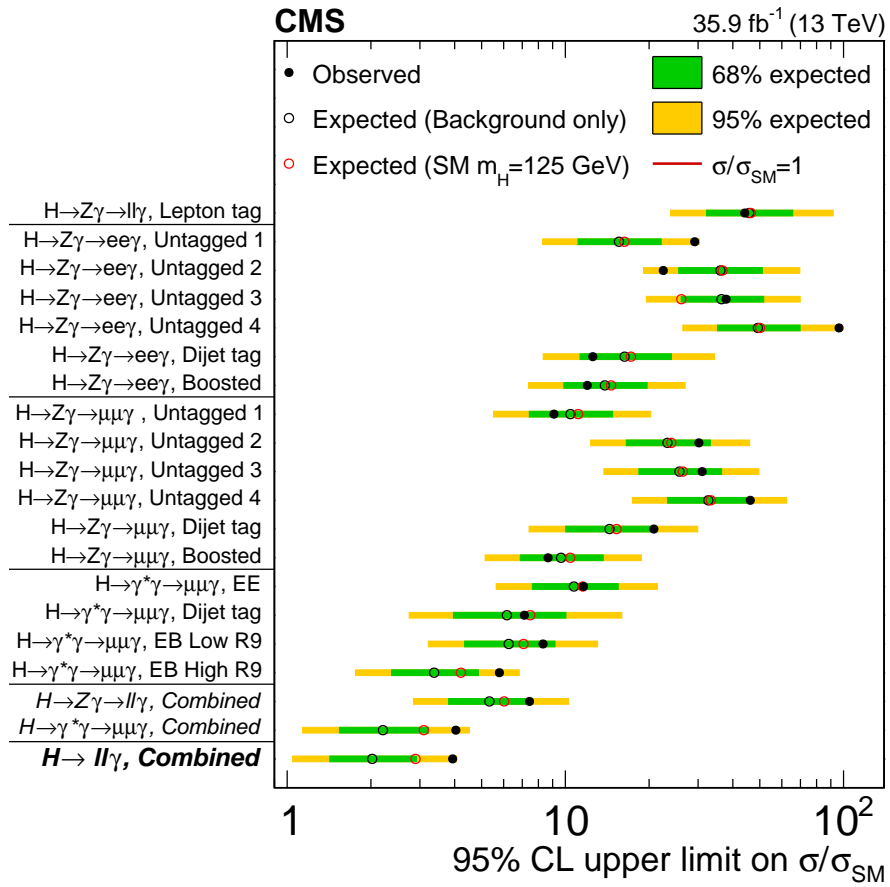


Figure 7: Exclusion limit, at 95% CL, on the cross section of $H \rightarrow \ell\ell\gamma$ relative to the SM prediction, for an SM Higgs boson of $m_H = 125$ GeV. The upper limits of each analysis category, as well as their combinations, are shown. Black full (empty) circles show the observed (background only expected) limit. Red circles show the expected upper limit assuming an SM Higgs boson decaying to $\ell\ell\gamma$ decay channel.

Acknowledgments

We congratulate our colleagues in the CERN accelerator departments for the excellent performance of the LHC and thank the technical and administrative staffs at CERN and at other CMS institutes for their contributions to the success of the CMS effort. In addition, we gratefully acknowledge the computing centres and personnel of the Worldwide LHC Computing Grid for delivering so effectively the computing infrastructure essential to our analyses. Finally, we acknowledge the enduring support for the construction and operation of the LHC and the CMS detector provided by the following funding agencies: BMWFW and FWF (Austria); FNRS and FWO (Belgium); CNPq, CAPES, FAPERJ, FAPERGS, and FAPESP (Brazil); MES (Bulgaria); CERN; CAS, MoST, and NSFC (China); COLCIENCIAS (Colombia); MSES and CSF (Croatia); RPF (Cyprus); SENESCYT (Ecuador); MoER, ERC IUT, and ERDF (Estonia); Academy of Finland, MEC, and HIP (Finland); CEA and CNRS/IN2P3 (France); BMBF, DFG, and HGF (Germany); GSRT (Greece); NKFI (Hungary); DAE and DST (India); IPM (Iran); SFI (Ireland); INFN (Italy); MSIP and NRF (Republic of Korea); LAS (Lithuania); MOE and UM (Malaysia); BUAP, CINVESTAV, CONACYT, LNS, SEP, and UASLP-FAI (Mexico); MBIE (New Zealand); PAEC (Pakistan); MSHE and NSC (Poland); FCT (Portugal); JINR (Dubna); MON, RosAtom, RAS, RFBR, and NRC KI (Russia); MESTD (Serbia); SEIDI, CPAN, PCTI, and FEDER (Spain); Swiss Funding Agencies (Switzerland); MST (Taipei); ThEPCenter, IPST, STAR, and NSTDA (Thailand); TUBITAK and TAEK (Turkey); NASU and SFFR (Ukraine); STFC (United Kingdom); DOE and NSF (USA).

Individuals have received support from the Marie-Curie programme and the European Research Council and Horizon 2020 Grant, contract No. 675440 (European Union); the Leventis Foundation; the A. P. Sloan Foundation; the Alexander von Humboldt Foundation; the Belgian Federal Science Policy Office; the Fonds pour la Formation à la Recherche dans l'Industrie et dans l'Agriculture (FRIA-Belgium); the Agentschap voor Innovatie door Wetenschap en Technologie (IWT-Belgium); the F.R.S.-FNRS and FWO (Belgium) under the "Excellence of Science - EOS" - be.h project n. 30820817; the Ministry of Education, Youth and Sports (MEYS) of the Czech Republic; the Lendület ("Momentum") Programme and the János Bolyai Research Scholarship of the Hungarian Academy of Sciences, the New National Excellence Program ÚNKP, the NKFI research grants 123842, 123959, 124845, 124850 and 125105 (Hungary); the Council of Science and Industrial Research, India; the HOMING PLUS programme of the Foundation for Polish Science, cofinanced from European Union, Regional Development Fund, the Mobility Plus programme of the Ministry of Science and Higher Education, the National Science Center (Poland), contracts Harmonia 2014/14/M/ST2/00428, Opus 2014/13/B/ST2/02543, 2014/15/B/ST2/03998, and 2015/19/B/ST2/02861, Sonata-bis 2012/07/E/ST2/01406; the National Priorities Research Program by Qatar National Research Fund; the Programa Estatal de Fomento de la Investigación Científica y Técnica de Excelencia María de Maeztu, grant MDM-2015-0509 and the Programa Severo Ochoa del Principado de Asturias; the Thalís and Aristeia programmes cofinanced by EU-ESF and the Greek NSRF; the Rachadapisek Sompot Fund for Postdoctoral Fellowship, Chulalongkorn University and the Chulalongkorn Academic into Its 2nd Century Project Advancement Project (Thailand); the Welch Foundation, contract C-1845; and the Weston Havens Foundation (USA).

References

- [1] A. Abbasabadi, D. Bowser-Chao, D. A. Dicus, and W. W. Repko, "Radiative Higgs boson decays $H \rightarrow ff\gamma$ ", *Phys. Rev. D* **55** (1997) 5647, doi:10.1103/PhysRevD.55.5647, arXiv:hep-ph/9611209.

-
- [2] L. B. Chen, C. F. Qiao, and R. L. Zhu, “Reconstructing the 125 GeV SM Higgs boson through $\ell\bar{\ell}\gamma$ ”, *Phys. Lett. B* **726** (2013) 306, doi:10.1016/j.physletb.2013.08.050, arXiv:1211.6058.
- [3] Y. Sun, H. Chang, and D. Gao, “Higgs decays to $\gamma\ell^+\ell^-$ in the standard model”, *JHEP* **05** (2013) 061, doi:10.1007/JHEP05(2013)061, arXiv:1303.2230.
- [4] G. Passarino, “Higgs boson production and decay: Dalitz sector”, *Phys. Lett. B* **727** (2013) 424, doi:10.1016/j.physletb.2013.10.052, arXiv:1308.0422.
- [5] M. Carena, I. Low, and C. E. M. Wagner, “Implications of a modified Higgs to diphoton decay width”, *JHEP* **08** (2012) 060, doi:10.1007/JHEP08(2012)060, arXiv:1206.1082.
- [6] C.-S. Chen, C.-Q. Geng, D. Huang, and L.-H. Tsai, “New scalar contributions to $H \rightarrow Z\gamma$ ”, *Phys. Rev. D* **87** (2013) 075019, doi:10.1103/PhysRevD.87.075019, arXiv:1301.4694.
- [7] I. Low, J. Lykken, and G. Shaughnessy, “Singlet scalars as Higgs imposters at the Large Hadron Collider”, *Phys. Rev. D* **84** (2011) 035027, doi:10.1103/PhysRevD.84.035027, arXiv:1105.4587.
- [8] M. Bauer, M. Neubert, and A. Thamm, “LHC as an axion factory: Probing an axion explanation for $(g-2)_\mu$ with exotic Higgs decays”, *Phys. Rev. Lett.* **119** (2017) 031802, doi:10.1103/PhysRevLett.119.031802, arXiv:1704.08207.
- [9] A. Korchin and V. Kovalchuk, “Angular distribution and forward-backward asymmetry of the Higgs-boson decay to photon and lepton pair”, *Eur. Phys. J. C* **74** (2014) 3141, doi:10.1140/epjc/s10052-014-3141-7, arXiv:1408.0342.
- [10] C.-W. Chiang and K. Yagyu, “Higgs boson decays to $\gamma\gamma$ and $Z\gamma$ in models with Higgs extensions”, *Phys. Rev. D* **87** (2013) 033003, doi:10.1103/PhysRevD.87.033003, arXiv:1207.1065.
- [11] S. Dawson and P. P. Giardino, “Higgs decays to ZZ and $Z\gamma$ in the standard model effective field theory: An NLO analysis”, *Phys. Rev. D* **97** (2018), no. 9, 093003, doi:10.1103/PhysRevD.97.093003, arXiv:1801.01136.
- [12] ATLAS and CMS Collaborations, “Combined measurement of the Higgs boson mass in pp collisions at $\sqrt{s} = 7$ and 8 TeV with the ATLAS and CMS experiments”, *Phys. Rev. Lett.* **114** (2015) 191803, doi:10.1103/PhysRevLett.114.191803, arXiv:1503.07589.
- [13] CMS Collaboration, “Measurements of properties of the Higgs boson decaying into the four-lepton final state in pp collisions at $\sqrt{s} = 13$ TeV”, *JHEP* **11** (2017) 047, doi:10.1007/JHEP11(2017)047, arXiv:1706.09936.
- [14] LHC Higgs Cross Section Working Group Collaboration, “Handbook of LHC Higgs cross sections: 4. deciphering the nature of the higgs sector”, (2016). arXiv:1610.07922.
- [15] J. M. Campbell and R. Ellis, “MCFM for the Tevatron and the LHC”, *Nucl. Phys. Proc. Suppl.* **205** (2010) 10, doi:10.1016/j.nuclphysbps.2010.08.011, arXiv:1007.3492.

- [16] D. A. Dicus and W. W. Repko, "Calculation of the decay $H \rightarrow e\bar{e}\gamma$ ", *Phys. Rev. D* **87** (2013) 077301, doi:10.1103/PhysRevD.87.077301, arXiv:1302.2159.
- [17] D. A. Dicus and W. W. Repko, "Dalitz decay $H \rightarrow f\bar{f}\gamma$ as a background for $H \rightarrow \gamma\gamma$ ", *Phys. Rev. D* **89** (2014) 093013, doi:10.1103/PhysRevD.89.093013, arXiv:1402.5317.
- [18] A. Firan and R. Stroynowski, "Internal conversions in Higgs decays to two photons", *Phys. Rev. D* **76** (2007) 057301, doi:10.1103/PhysRevD.76.057301, arXiv:0704.3987.
- [19] ATLAS Collaboration, "Search for Higgs boson decays to a photon and a Z boson in pp collisions at $\sqrt{s} = 7$ and 8 TeV with the ATLAS detector", *Phys. Lett. B* **732** (2014) 8, doi:10.1016/j.physletb.2014.03.015, arXiv:1402.3051.
- [20] CMS Collaboration, "Search for a Higgs boson decaying into a Z and a photon in pp collisions at $\sqrt{s} = 7$ and 8 TeV", *Phys. Lett. B* **726** (2013) 587, doi:10.1016/j.physletb.2013.09.057, arXiv:1307.5515.
- [21] CMS Collaboration, "Search for a Higgs boson decaying into $\gamma^*\gamma \rightarrow \ell\ell\gamma$ with low dilepton mass in pp collisions at $\sqrt{s} = 8$ TeV", *Phys. Lett. B* **753** (2016) 341, doi:10.1016/j.physletb.2015.12.039, arXiv:1507.03031.
- [22] ATLAS Collaboration, "Searches for the $Z\gamma$ decay mode of the Higgs boson and for new high-mass resonances in pp collisions at $\sqrt{s} = 13$ TeV with the ATLAS detector", *JHEP* **10** (2017) 112, doi:10.1007/JHEP10(2017)112, arXiv:1708.00212.
- [23] CMS Collaboration, "The CMS experiment at the CERN LHC", *JINST* **3** (2008) S08004, doi:10.1088/1748-0221/3/08/S08004.
- [24] CMS Collaboration, "The CMS trigger system", *JINST* **12** (2017) P01020, doi:10.1088/1748-0221/12/01/P01020, arXiv:1609.02366.
- [25] CMS Collaboration, "Particle-flow reconstruction and global event description with the CMS detector", *JINST* **12** (2017) P10003, doi:10.1088/1748-0221/12/10/P10003, arXiv:1706.04965.
- [26] CMS Collaboration, "Performance of photon reconstruction and identification with the CMS detector in proton-proton collisions at $\sqrt{s} = 8$ TeV", *JINST* **10** (2015) P08010, doi:10.1088/1748-0221/10/08/P08010, arXiv:1502.02702.
- [27] CMS Collaboration, "Measurement of the inclusive W and Z production cross sections in pp collisions at $\sqrt{s} = 7$ TeV", *JHEP* **10** (2011) 132, doi:10.1007/JHEP10(2011)132, arXiv:1107.4789.
- [28] M. Cacciari, G. P. Salam, and G. Soyez, "Fastjet user manual", *Eur. Phys. J. C* **72** (2012) 1896, doi:10.1140/epjc/s10052-012-1896-2, arXiv:1111.6097.
- [29] M. Cacciari and G. P. Salam, "Pileup subtraction using jet areas", *Phys. Lett. B* **659** (2008) 119, doi:10.1016/j.physletb.2007.09.077, arXiv:0707.1378.
- [30] M. Cacciari, G. P. Salam, and G. Soyez, "The catchment area of jets", *JHEP* **04** (2008) 005, doi:10.1088/1126-6708/2008/04/005, arXiv:0802.1188.

-
- [31] D. L. Rainwater, R. Szalapski, and D. Zeppenfeld, “Probing color singlet exchange in $z +$ two jet events at the CERN LHC”, *Phys. Rev. D* **54** (1996) 6680, doi:10.1103/PhysRevD.54.6680, arXiv:hep-ph/9605444.
- [32] Particle Data Group Collaboration, “Review of particle physics”, *Chin. Phys. C* **40** (2016), no. 10, 100001, doi:10.1088/1674-1137/40/10/100001.
- [33] J. Alwall et al., “The automated computation of tree-level and next-to-leading order differential cross sections, and their matching to parton shower simulations”, *JHEP* **07** (2014) 079, doi:10.1007/JHEP07(2014)079, arXiv:1405.0301.
- [34] NNPDF Collaboration, “Parton distributions for the LHC run II”, *JHEP* **04** (2015) 040, doi:10.1007/JHEP04(2015)040, arXiv:1410.8849.
- [35] CMS Collaboration, “Event generator tunes obtained from underlying event and multiparton scattering measurements”, *Eur. Phys. J. C* **76** (2016) 155, doi:10.1140/epjc/s10052-016-3988-x, arXiv:1512.00815.
- [36] T. Sjöstrand, S. Mrenna, and P. Z. Skands, “A brief introduction to PYTHIA 8.1”, *Comput. Phys. Commun.* **178** (2008) 852, doi:10.1016/j.cpc.2008.01.036, arXiv:0710.3820.
- [37] T. Sjöstrand et al., “An introduction to PYTHIA 8.2”, *Comput. Phys. Commun.* **191** (2015) 159, doi:10.1016/j.cpc.2015.01.024, arXiv:1410.3012.
- [38] P. Artoisenet et al., “A framework for Higgs characterisation”, *JHEP* **11** (2013) 043, doi:10.1007/JHEP11(2013)043, arXiv:1306.6464.
- [39] P. de Aquino and K. Mawatari, “Characterising a Higgs-like resonance at the LHC”, in *Proceedings, 1st Toyama International Workshop on Higgs as a Probe of New Physics 2013 (HPNP2013): Toyama, Japan, February 13-16, 2013*. 2013. arXiv:1307.5607.
- [40] S. Alioli, P. Nason, C. Oleari, and E. Re, “NLO Higgs boson production via gluon fusion matched with shower in POWHEG”, *JHEP* **04** (2009) 002, doi:10.1088/1126-6708/2009/04/002, arXiv:0812.0578.
- [41] P. Nason and C. Oleari, “NLO Higgs boson production via vector-boson fusion matched with shower in POWHEG”, *JHEP* **02** (2010) 037, doi:10.1007/JHEP02(2010)037, arXiv:0911.5299.
- [42] M. J. Oreglia, “A study of the reactions $\psi' \rightarrow \gamma\gamma\psi$ ”. PhD thesis, Stanford University, 1980. SLAC Report SLAC-R-236, see Appendix D.
- [43] A. L. Read, “Presentation of search results: The CL_s technique”, *J. Phys. G* **28** (2002) 2693, doi:10.1088/0954-3899/28/10/313.
- [44] T. Junk, “Confidence level computation for combining searches with small statistics”, *Nucl. Instrum. Meth. A* **434** (1999) 435, doi:10.1016/S0168-9002(99)00498-2, arXiv:hep-ex/9902006.
- [45] ATLAS and CMS Collaborations, The LHC Higgs combination group, “Procedure for the LHC Higgs boson search combination in summer 2011”, Technical Report CMS-NOTE-2011-005. ATL-PHYS-PUB-2011-11, 2011.

- [46] G. Cowan, K. Cranmer, E. Gross, and O. Vitells, “Asymptotic formulae for likelihood-based tests of new physics”, *Eur. Phys. J. C* **71** (2011) 1554, doi:10.1140/epjc/s10052-011-1554-0, arXiv:1007.1727. [Erratum: doi:10.1140/epjc/s10052-013-2501-z].
- [47] CMS Collaboration, “CMS luminosity measurements for the 2016 data taking period”, CMS Physics Analysis Summary CMS-PAS-LUM-17-001, 2017.
- [48] CMS Collaboration, “Measurement of the inelastic proton-proton cross section at $\sqrt{s} = 13$ TeV”, (2018). arXiv:1802.02613.
- [49] A. D. Martin, W. J. Stirling, R. S. Thorne, and G. Watt, “Parton distributions for the LHC”, *Eur. Phys. J. C* **63** (2009) 189, doi:10.1140/epjc/s10052-009-1072-5, arXiv:0901.0002.
- [50] H. Lai et al., “New parton distributions for collider physics”, *Phys. Rev. D* **82** (2010) 74024, doi:10.1103/PhysRevD.82.074024, arXiv:1007.2241.
- [51] J. Butterworth et al., “PDF4LHC recommendations for LHC run II”, *J. Phys. G* **43** (2016) 023001, doi:10.1088/0954-3899/43/2/023001, arXiv:1510.03865.

A The CMS Collaboration

Yerevan Physics Institute, Yerevan, Armenia

A.M. Sirunyan, A. Tumasyan

Institut für Hochenergiephysik, Wien, Austria

W. Adam, F. Ambrogio, E. Asilar, T. Bergauer, J. Brandstetter, E. Brondolin, M. Dragicevic, J. Erö, A. Escalante Del Valle, M. Flechl, R. Frühwirth¹, V.M. Ghete, J. Hrubec, M. Jeitler¹, N. Krammer, I. Krätschmer, D. Liko, T. Madlener, I. Mikulec, N. Rad, H. Rohringer, J. Schieck¹, R. Schöfbeck, M. Spanring, D. Spitzbart, A. Taurok, W. Waltenberger, J. Wittmann, C.-E. Wulz¹, M. Zarucki

Institute for Nuclear Problems, Minsk, Belarus

V. Chekhovsky, V. Mossolov, J. Suarez Gonzalez

Universiteit Antwerpen, Antwerpen, Belgium

E.A. De Wolf, D. Di Croce, X. Janssen, J. Lauwers, M. Pieters, M. Van De Klundert, H. Van Haevermaet, P. Van Mechelen, N. Van Remortel

Vrije Universiteit Brussel, Brussel, Belgium

S. Abu Zeid, F. Blekman, J. D'Hondt, I. De Bruyn, J. De Clercq, K. Deroover, G. Flouris, D. Lontkovskyi, S. Lowette, I. Marchesini, S. Moortgat, L. Moreels, Q. Python, K. Skovpen, S. Tavernier, W. Van Doninck, P. Van Mulders, I. Van Parijs

Université Libre de Bruxelles, Bruxelles, Belgium

D. Beghin, B. Bilin, H. Brun, B. Clerboux, G. De Lentdecker, H. Delannoy, B. Dorney, G. Fasanella, L. Favart, R. Goldouzian, A. Grebenyuk, A.K. Kalsi, T. Lenzi, J. Luetic, N. Postiau, E. Starling, L. Thomas, C. Vander Velde, P. Vanlaer, D. Vannerom, Q. Wang

Ghent University, Ghent, Belgium

T. Cornelis, D. Dobur, A. Fagot, M. Gul, I. Khvastunov², D. Poyraz, C. Roskas, D. Trocino, M. Tytgat, W. Verbeke, B. Vermassen, M. Vit, N. Zaganidis

Université Catholique de Louvain, Louvain-la-Neuve, Belgium

H. Bakhshiansohi, O. Bondu, S. Brochet, G. Bruno, C. Caputo, P. David, C. Delaere, M. Delcourt, B. Francois, A. Giammanco, G. Krintiras, V. Lemaitre, A. Magitteri, A. Mertens, M. Musich, K. Piotrkowski, A. Saggio, M. Vidal Marono, S. Wertz, J. Zobec

Centro Brasileiro de Pesquisas Fisicas, Rio de Janeiro, Brazil

F.L. Alves, G.A. Alves, L. Brito, G. Correia Silva, C. Hensel, A. Moraes, M.E. Pol, P. Rebello Teles

Universidade do Estado do Rio de Janeiro, Rio de Janeiro, Brazil

E. Belchior Batista Das Chagas, W. Carvalho, J. Chinellato³, E. Coelho, E.M. Da Costa, G.G. Da Silveira⁴, D. De Jesus Damiao, C. De Oliveira Martins, S. Fonseca De Souza, H. Malbouisson, D. Matos Figueiredo, M. Melo De Almeida, C. Mora Herrera, L. Mundim, H. Nogima, W.L. Prado Da Silva, L.J. Sanchez Rosas, A. Santoro, A. Sznajder, M. Thiel, E.J. Tonelli Manganote³, F. Torres Da Silva De Araujo, A. Vilela Pereira

Universidade Estadual Paulista ^a, Universidade Federal do ABC ^b, São Paulo, Brazil

S. Ahuja^a, C.A. Bernardes^a, L. Calligaris^a, T.R. Fernandez Perez Tomei^a, E.M. Gregores^b, P.G. Mercadante^b, S.F. Novaes^a, SandraS. Padula^a, D. Romero Abad^b

Institute for Nuclear Research and Nuclear Energy, Bulgarian Academy of Sciences, Sofia, Bulgaria

A. Aleksandrov, R. Hadjiiska, P. Iaydjiev, A. Marinov, M. Misheva, M. Rodozov, M. Shopova, G. Sultanov

University of Sofia, Sofia, Bulgaria

A. Dimitrov, L. Litov, B. Pavlov, P. Petkov

Beihang University, Beijing, China

W. Fang⁵, X. Gao⁵, L. Yuan

Institute of High Energy Physics, Beijing, China

M. Ahmad, J.G. Bian, G.M. Chen, H.S. Chen, M. Chen, Y. Chen, C.H. Jiang, D. Leggat, H. Liao, Z. Liu, F. Romeo, S.M. Shaheen, A. Spiezia, J. Tao, C. Wang, Z. Wang, E. Yazgan, H. Zhang, J. Zhao

State Key Laboratory of Nuclear Physics and Technology, Peking University, Beijing, China

Y. Ban, G. Chen, A. Levin, J. Li, L. Li, Q. Li, Y. Mao, S.J. Qian, D. Wang, Z. Xu

Tsinghua University, Beijing, China

Y. Wang

Universidad de Los Andes, Bogota, Colombia

C. Avila, A. Cabrera, C.A. Carrillo Montoya, L.F. Chaparro Sierra, C. Florez, C.F. González Hernández, M.A. Segura Delgado

University of Split, Faculty of Electrical Engineering, Mechanical Engineering and Naval Architecture, Split, Croatia

B. Courbon, N. Godinovic, D. Lelas, I. Puljak, T. Sculac

University of Split, Faculty of Science, Split, Croatia

Z. Antunovic, M. Kovac

Institute Rudjer Boskovic, Zagreb, Croatia

V. Brigljevic, D. Ferencek, K. Kadija, B. Mesic, A. Starodumov⁶, T. Susa

University of Cyprus, Nicosia, Cyprus

M.W. Ather, A. Attikis, M. Kolosova, G. Mavromanolakis, J. Mousa, C. Nicolaou, F. Ptochos, P.A. Razis, H. Rykaczewski

Charles University, Prague, Czech Republic

M. Finger⁷, M. Finger Jr.⁷

Escuela Politecnica Nacional, Quito, Ecuador

E. Ayala

Universidad San Francisco de Quito, Quito, Ecuador

E. Carrera Jarrin

Academy of Scientific Research and Technology of the Arab Republic of Egypt, Egyptian Network of High Energy Physics, Cairo, Egypt

H. Abdalla⁸, A.A. Abdelalim^{9,10}, A. Mohamed¹⁰

National Institute of Chemical Physics and Biophysics, Tallinn, Estonia

S. Bhowmik, A. Carvalho Antunes De Oliveira, R.K. Dewanjee, K. Ehataht, M. Kadastik, M. Raidal, C. Veelken

Department of Physics, University of Helsinki, Helsinki, Finland

P. Eerola, H. Kirschenmann, J. Pekkanen, M. Voutilainen

Helsinki Institute of Physics, Helsinki, Finland

J. Havukainen, J.K. Heikkilä, T. Järvinen, V. Karimäki, R. Kinnunen, T. Lampén, K. Lassila-Perini, S. Laurila, S. Lehti, T. Lindén, P. Luukka, T. Mäenpää, H. Siikonen, E. Tuominen, J. Tuominiemi

Lappeenranta University of Technology, Lappeenranta, Finland

T. Tuuva

IRFU, CEA, Université Paris-Saclay, Gif-sur-Yvette, France

M. Besancon, F. Couderc, M. Dejardin, D. Denegri, J.L. Faure, F. Ferri, S. Ganjour, A. Givernaud, P. Gras, G. Hamel de Monchenault, P. Jarry, C. Leloup, E. Locci, J. Malcles, G. Negro, J. Rander, A. Rosowsky, M.Ö. Sahin, M. Titov

Laboratoire Leprince-Ringuet, Ecole polytechnique, CNRS/IN2P3, Université Paris-Saclay, Palaiseau, France

A. Abdulsalam¹¹, C. Amendola, I. Antropov, F. Beaudette, P. Busson, C. Charlot, R. Granier de Cassagnac, I. Kucher, S. Lisniak, A. Lobanov, J. Martin Blanco, M. Nguyen, C. Ochando, G. Ortona, P. Pigard, R. Salerno, J.B. Sauvan, Y. Sirois, A.G. Stahl Leiton, A. Zabi, A. Zghiche

Université de Strasbourg, CNRS, IPHC UMR 7178, Strasbourg, France

J.-L. Agram¹², J. Andrea, D. Bloch, J.-M. Brom, E.C. Chabert, V. Cherepanov, C. Collard, E. Conte¹², J.-C. Fontaine¹², D. Gelé, U. Goerlach, M. Jansová, A.-C. Le Bihan, N. Tonon, P. Van Hove

Centre de Calcul de l'Institut National de Physique Nucleaire et de Physique des Particules, CNRS/IN2P3, Villeurbanne, France

S. Gadrat

Université de Lyon, Université Claude Bernard Lyon 1, CNRS-IN2P3, Institut de Physique Nucléaire de Lyon, Villeurbanne, France

S. Beauceron, C. Bernet, G. Boudoul, N. Chanon, R. Chierici, D. Contardo, P. Depasse, H. El Mamouni, J. Fay, L. Finco, S. Gascon, M. Gouzevitch, G. Grenier, B. Ille, F. Lagarde, I.B. Laktineh, H. Lattaud, M. Lethuillier, L. Mirabito, A.L. Pequegnot, S. Perries, A. Popov¹³, V. Sordini, M. Vander Donckt, S. Viret, S. Zhang

Georgian Technical University, Tbilisi, Georgia

A. Khvedelidze⁷

Tbilisi State University, Tbilisi, Georgia

Z. Tsamalaidze⁷

RWTH Aachen University, I. Physikalisches Institut, Aachen, Germany

C. Autermann, L. Feld, M.K. Kiesel, K. Klein, M. Lipinski, M. Preuten, M.P. Rauch, C. Schomakers, J. Schulz, M. Teroerde, B. Wittmer, V. Zhukov¹³

RWTH Aachen University, III. Physikalisches Institut A, Aachen, Germany

A. Albert, D. Duchardt, M. Endres, M. Erdmann, T. Esch, R. Fischer, S. Ghosh, A. Güth, T. Hebbeker, C. Heidemann, K. Hoepfner, H. Keller, S. Knutzen, L. Mastrolorenzo, M. Merschmeyer, A. Meyer, P. Millet, S. Mukherjee, T. Pook, M. Radziej, H. Reithler, M. Rieger, F. Scheuch, A. Schmidt, D. Teyssier

RWTH Aachen University, III. Physikalisches Institut B, Aachen, Germany

G. Flügge, O. Hlushchenko, B. Kargoll, T. Kress, A. Künsken, T. Müller, A. Nehr Korn, A. Nowack, C. Pistone, O. Pooth, H. Sert, A. Stahl¹⁴

Deutsches Elektronen-Synchrotron, Hamburg, Germany

M. Aldaya Martin, T. Arndt, C. Asawatangtrakuldee, I. Babounikau, K. Beernaert, O. Behnke, U. Behrens, A. Bermúdez Martínez, D. Bertsche, A.A. Bin Anuar, K. Borras¹⁵, V. Botta, A. Campbell, P. Connor, C. Contreras-Campana, F. Costanza, V. Danilov, A. De Wit, M.M. Defranchis, C. Diez Pardos, D. Domínguez Damiani, G. Eckerlin, T. Eichhorn, A. Elwood, E. Eren, E. Gallo¹⁶, A. Geiser, J.M. Grados Luyando, A. Grohsjean, P. Gunnellini, M. Guthoff, M. Haranko, A. Harb, J. Hauk, H. Jung, M. Kasemann, J. Keaveney, C. Kleinwort, J. Knolle, D. Krücker, W. Lange, A. Lelek, T. Lenz, K. Lipka, W. Lohmann¹⁷, R. Mankel, I.-A. Melzer-Pellmann, A.B. Meyer, M. Meyer, M. Missiroli, G. Mittag, J. Mnich, V. Myronenko, S.K. Pflitsch, D. Pitzl, A. Raspereza, M. Savitskyi, P. Saxena, P. Schütze, C. Schwanenberger, R. Shevchenko, A. Singh, N. Stefaniuk, H. Tholen, A. Vagnerini, G.P. Van Onsem, R. Walsh, Y. Wen, K. Wichmann, C. Wissing, O. Zenaiev

University of Hamburg, Hamburg, Germany

R. Aggleton, S. Bein, L. Benato, A. Benecke, V. Blobel, M. Centis Vignali, T. Dreyer, E. Garutti, D. Gonzalez, J. Haller, A. Hinzmann, A. Karavdina, G. Kasieczka, R. Klanner, R. Kogler, N. Kovalchuk, S. Kurz, V. Kutzner, J. Lange, D. Marconi, J. Multhaup, M. Niedziela, D. Nowatschin, A. Perieanu, A. Reimers, O. Rieger, C. Scharf, P. Schleper, S. Schumann, J. Schwandt, J. Sonneveld, H. Stadie, G. Steinbrück, F.M. Stober, M. Stöver, D. Troendle, A. Vanhoefer, B. Vormwald

Karlsruher Institut fuer Technology

M. Akbiyik, C. Barth, M. Baselga, S. Baur, E. Butz, R. Caspart, T. Chwalek, F. Colombo, W. De Boer, A. Dierlamm, N. Faltermann, B. Freund, M. Giffels, M.A. Harrendorf, F. Hartmann¹⁴, S.M. Heindl, U. Husemann, F. Kassel¹⁴, I. Katkov¹³, S. Kudella, H. Mildner, S. Mitra, M.U. Mozer, Th. Müller, M. Plagge, G. Quast, K. Rabbertz, M. Schröder, I. Shvetsov, G. Sieber, H.J. Simonis, R. Ulrich, S. Wayand, M. Weber, T. Weiler, S. Williamson, C. Wöhrmann, R. Wolf

Institute of Nuclear and Particle Physics (INPP), NCSR Demokritos, Aghia Paraskevi, Greece

G. Anagnostou, G. Daskalakis, T. Gerasis, A. Kyriakis, D. Loukas, G. Paspalaki, I. Topsis-Giotis

National and Kapodistrian University of Athens, Athens, Greece

G. Karathanasis, S. Kesisoglou, P. Kontaxakis, A. Panagiotou, N. Saoulidou, E. Tziaferi, K. Vellidis

National Technical University of Athens, Athens, Greece

K. Kousouris, I. Papakrivopoulos, G. Tsipolitis

University of Ioánnina, Ioánnina, Greece

I. Evangelou, C. Foudas, P. Giannelis, P. Katsoulis, P. Kokkas, S. Mallios, N. Manthos, I. Papadopoulos, E. Paradas, J. Strologas, F.A. Triantis, D. Tsitsonis

MTA-ELTE Lendület CMS Particle and Nuclear Physics Group, Eötvös Loránd University, Budapest, Hungary

M. Bartók¹⁸, M. Csanad, N. Filipovic, P. Major, M.I. Nagy, G. Pasztor, O. Surányi, G.I. Veres

Wigner Research Centre for Physics, Budapest, Hungary

G. Bencze, C. Hajdu, D. Horvath¹⁹, Á. Hunyadi, F. Sikler, T.Á. Vámi, V. Veszpremi, G. Vesztergombi[†]

Institute of Nuclear Research ATOMKI, Debrecen, Hungary

N. Beni, S. Czellar, J. Karacsi²⁰, A. Makovec, J. Molnar, Z. Szillasi

Institute of Physics, University of Debrecen, Debrecen, Hungary

P. Raics, Z.L. Trocsanyi, B. Ujvari

Indian Institute of Science (IISc), Bangalore, India

S. Choudhury, J.R. Komaragiri, P.C. Tiwari

National Institute of Science Education and Research, HBNI, Bhubaneswar, IndiaS. Bahinipati²¹, C. Kar, P. Mal, K. Mandal, A. Nayak²², D.K. Sahoo²¹, S.K. Swain**Panjab University, Chandigarh, India**

S. Bansal, S.B. Beri, V. Bhatnagar, S. Chauhan, R. Chawla, N. Dhingra, R. Gupta, A. Kaur, A. Kaur, M. Kaur, S. Kaur, R. Kumar, P. Kumari, M. Lohan, A. Mehta, K. Sandeep, S. Sharma, J.B. Singh, G. Walia

University of Delhi, Delhi, India

A. Bhardwaj, B.C. Choudhary, R.B. Garg, M. Gola, S. Keshri, Ashok Kumar, S. Malhotra, M. Naimuddin, P. Priyanka, K. Ranjan, Aashaq Shah, R. Sharma

Saha Institute of Nuclear Physics, HBNI, Kolkata, IndiaR. Bhardwaj²³, M. Bharti, R. Bhattacharya, S. Bhattacharya, U. Bhawandeep²³, D. Bhowmik, S. Dey, S. Dutt²³, S. Dutta, S. Ghosh, K. Mondal, S. Nandan, A. Purohit, P.K. Rout, A. Roy, S. Roy Chowdhury, S. Sarkar, M. Sharan, B. Singh, S. Thakur²³**Indian Institute of Technology Madras, Madras, India**

P.K. Behera

Bhabha Atomic Research Centre, Mumbai, India

R. Chudasama, D. Dutta, V. Jha, V. Kumar, P.K. Netrakanti, L.M. Pant, P. Shukla

Tata Institute of Fundamental Research-A, Mumbai, India

T. Aziz, M.A. Bhat, S. Dugad, G.B. Mohanty, N. Sur, B. Sutar, RavindraKumar Verma

Tata Institute of Fundamental Research-B, Mumbai, IndiaS. Banerjee, S. Bhattacharya, S. Chatterjee, P. Das, M. Guchait, Sa. Jain, S. Karmakar, S. Kumar, M. Maity²⁴, G. Majumder, K. Mazumdar, N. Sahoo, T. Sarkar²⁴**Indian Institute of Science Education and Research (IISER), Pune, India**

S. Chauhan, S. Dube, V. Hegde, A. Kapoor, K. Kothekar, S. Pandey, A. Rane, S. Sharma

Institute for Research in Fundamental Sciences (IPM), Tehran, IranS. Chenarani²⁵, E. Eskandari Tadavani, S.M. Etesami²⁵, M. Khakzad, M. Mohammadi Najafabadi, M. Naseri, F. Rezaei Hosseinabadi, B. Safarzadeh²⁶, M. Zeinali**University College Dublin, Dublin, Ireland**

M. Felcini, M. Grunewald

INFN Sezione di Bari ^a, Università di Bari ^b, Politecnico di Bari ^c, Bari, ItalyM. Abbrescia^{a,b}, C. Calabria^{a,b}, A. Colaleo^a, D. Creanza^{a,c}, L. Cristella^{a,b}, N. De Filippis^{a,c}, M. De Palma^{a,b}, A. Di Florio^{a,b}, F. Errico^{a,b}, L. Fiore^a, A. Gelmi^{a,b}, G. Iaselli^{a,c}, S. Lezki^{a,b}, G. Maggi^{a,c}, M. Maggi^a, G. Miniello^{a,b}, S. My^{a,b}, S. Nuzzo^{a,b}, A. Pompili^{a,b}, G. Pugliese^{a,c}, R. Radogna^a, A. Ranieri^a, G. Selvaggi^{a,b}, A. Sharma^a, L. Silvestris^{a,14}, R. Venditti^a, P. Verwilligen^a, G. Zito^a**INFN Sezione di Bologna ^a, Università di Bologna ^b, Bologna, Italy**G. Abbiendi^a, C. Battilana^{a,b}, D. Bonacorsi^{a,b}, L. Borgonovi^{a,b}, S. Braibant-Giacomelli^{a,b}, R. Campanini^{a,b}, P. Capiluppi^{a,b}, A. Castro^{a,b}, F.R. Cavallo^a, S.S. Chhibra^{a,b}, C. Ciocca^a,

G. Codispoti^{a,b}, M. Cuffiani^{a,b}, G.M. Dallavalle^a, F. Fabbri^a, A. Fanfani^{a,b}, P. Giacomelli^a, C. Grandi^a, L. Guiducci^{a,b}, F. Iemmi^{a,b}, S. Marcellini^a, G. Masetti^a, A. Montanari^a, F.L. Navarria^{a,b}, A. Perrotta^a, F. Primavera^{a,b,14}, A.M. Rossi^{a,b}, T. Rovelli^{a,b}, G.P. Siroli^{a,b}, N. Tosi^a

INFN Sezione di Catania^a, Università di Catania^b, Catania, Italy

S. Albergo^{a,b}, A. Di Mattia^a, R. Potenza^{a,b}, A. Tricomi^{a,b}, C. Tuve^{a,b}

INFN Sezione di Firenze^a, Università di Firenze^b, Firenze, Italy

G. Barbagli^a, K. Chatterjee^{a,b}, V. Ciulli^{a,b}, C. Civinini^a, R. D'Alessandro^{a,b}, E. Focardi^{a,b}, G. Latino, P. Lenzi^{a,b}, M. Meschini^a, S. Paoletti^a, L. Russo^{a,27}, G. Sguazzoni^a, D. Strom^a, L. Viliani^a

INFN Laboratori Nazionali di Frascati, Frascati, Italy

L. Benussi, S. Bianco, F. Fabbri, D. Piccolo

INFN Sezione di Genova^a, Università di Genova^b, Genova, Italy

F. Ferro^a, F. Ravera^{a,b}, E. Robutti^a, S. Tosi^{a,b}

INFN Sezione di Milano-Bicocca^a, Università di Milano-Bicocca^b, Milano, Italy

A. Benaglia^a, A. Beschi^b, L. Brianza^{a,b}, F. Brivio^{a,b}, V. Ciriolo^{a,b,14}, S. Di Guida^{a,d,14}, M.E. Dinardo^{a,b}, S. Fiorendi^{a,b}, S. Gennai^a, A. Ghezzi^{a,b}, P. Govoni^{a,b}, M. Malberti^{a,b}, S. Malvezzi^a, A. Massironi^{a,b}, D. Menasce^a, L. Moroni^a, M. Paganoni^{a,b}, D. Pedrini^a, S. Ragazzi^{a,b}, T. Tabarelli de Fatis^{a,b}

INFN Sezione di Napoli^a, Università di Napoli 'Federico II'^b, Napoli, Italy, Università della Basilicata^c, Potenza, Italy, Università G. Marconi^d, Roma, Italy

S. Buontempo^a, N. Cavallo^{a,c}, A. Di Crescenzo^{a,b}, F. Fabozzi^{a,c}, F. Fienga^a, G. Galati^a, A.O.M. Iorio^{a,b}, W.A. Khan^a, L. Lista^a, S. Meola^{a,d,14}, P. Paolucci^{a,14}, C. Sciacca^{a,b}, E. Voevodina^{a,b}

INFN Sezione di Padova^a, Università di Padova^b, Padova, Italy, Università di Trento^c, Trento, Italy

P. Azzi^a, N. Bacchetta^a, D. Bisello^{a,b}, A. Boletti^{a,b}, A. Bragagnolo, P. Checchia^a, M. Dall'Osso^{a,b}, P. De Castro Manzano^a, T. Dorigo^a, U. Dosselli^a, U. Gasparini^{a,b}, A. Gozzelino^a, S. Lacaprara^a, P. Lujan, M. Margoni^{a,b}, A.T. Meneguzzo^{a,b}, N. Pozzobon^{a,b}, P. Ronchese^{a,b}, R. Rossin^{a,b}, F. Simonetto^{a,b}, A. Tiko, E. Torassa^a, S. Ventura^a, M. Zanetti^{a,b}, P. Zotto^{a,b}, G. Zumerle^{a,b}

INFN Sezione di Pavia^a, Università di Pavia^b, Pavia, Italy

A. Braghieri^a, A. Magnani^a, P. Montagna^{a,b}, S.P. Ratti^{a,b}, V. Re^a, M. Ressegotti^{a,b}, C. Riccardi^{a,b}, P. Salvini^a, I. Vai^{a,b}, P. Vitulo^{a,b}

INFN Sezione di Perugia^a, Università di Perugia^b, Perugia, Italy

L. Alunni Solestizi^{a,b}, M. Biasini^{a,b}, G.M. Bilei^a, C. Cecchi^{a,b}, D. Ciangottini^{a,b}, L. Fanò^{a,b}, P. Lariccia^{a,b}, E. Manoni^a, G. Mantovani^{a,b}, V. Mariani^{a,b}, M. Menichelli^a, A. Rossi^{a,b}, A. Santocchia^{a,b}, D. Spiga^a

INFN Sezione di Pisa^a, Università di Pisa^b, Scuola Normale Superiore di Pisa^c, Pisa, Italy

K. Androsov^a, P. Azzurri^a, G. Bagliesi^a, L. Bianchini^a, T. Boccali^a, L. Borrello, R. Castaldi^a, M.A. Ciocci^{a,b}, R. Dell'Orso^a, G. Fedì^a, F. Fiori^{a,c}, L. Giannini^{a,c}, A. Giassi^a, M.T. Grippo^a, F. Ligabue^{a,c}, E. Manca^{a,c}, G. Mandorli^{a,c}, A. Messineo^{a,b}, F. Palla^a, A. Rizzi^{a,b}, P. Spagnolo^a, R. Tenchini^a, G. Tonelli^{a,b}, A. Venturi^a, P.G. Verdini^a

INFN Sezione di Roma^a, Sapienza Università di Roma^b, Rome, Italy

L. Barone^{a,b}, F. Cavallari^a, M. Cipriani^{a,b}, N. Daci^a, D. Del Re^{a,b}, E. Di Marco^{a,b}, M. Diemoz^a,

S. Gelli^{a,b}, E. Longo^{a,b}, B. Marzocchi^{a,b}, P. Meridiani^a, G. Organtini^{a,b}, F. Pandolfi^a, R. Paramatti^{a,b}, F. Preiato^{a,b}, S. Rahatlou^{a,b}, C. Rovelli^a, F. Santanastasio^{a,b}

INFN Sezione di Torino ^a, Università di Torino ^b, Torino, Italy, Università del Piemonte Orientale ^c, Novara, Italy

N. Amapane^{a,b}, R. Arcidiacono^{a,c}, S. Argiro^{a,b}, M. Arneodo^{a,c}, N. Bartosik^a, R. Bellan^{a,b}, C. Biino^a, N. Cartiglia^a, F. Cenna^{a,b}, S. Cometti, M. Costa^{a,b}, R. Covarelli^{a,b}, N. Demaria^a, B. Kiani^{a,b}, C. Mariotti^a, S. Maselli^a, E. Migliore^{a,b}, V. Monaco^{a,b}, E. Monteil^{a,b}, M. Monteno^a, M.M. Obertino^{a,b}, L. Pacher^{a,b}, N. Pastrone^a, M. Pelliccioni^a, G.L. Pinna Angioni^{a,b}, A. Romero^{a,b}, M. Ruspa^{a,c}, R. Sacchi^{a,b}, K. Shchelina^{a,b}, V. Sola^a, A. Solano^{a,b}, D. Soldi, A. Staiano^a

INFN Sezione di Trieste ^a, Università di Trieste ^b, Trieste, Italy

S. Belforte^a, V. Candelise^{a,b}, M. Casarsa^a, F. Cossutti^a, G. Della Ricca^{a,b}, F. Vazzoler^{a,b}, A. Zanetti^a

Kyungpook National University

D.H. Kim, G.N. Kim, M.S. Kim, J. Lee, S. Lee, S.W. Lee, C.S. Moon, Y.D. Oh, S. Sekmen, D.C. Son, Y.C. Yang

Chonnam National University, Institute for Universe and Elementary Particles, Kwangju, Korea

H. Kim, D.H. Moon, G. Oh

Hanyang University, Seoul, Korea

J. Goh, T.J. Kim

Korea University, Seoul, Korea

S. Cho, S. Choi, Y. Go, D. Gyun, S. Ha, B. Hong, Y. Jo, K. Lee, K.S. Lee, S. Lee, J. Lim, S.K. Park, Y. Roh

Sejong University, Seoul, Korea

H.S. Kim

Seoul National University, Seoul, Korea

J. Almond, J. Kim, J.S. Kim, H. Lee, K. Lee, K. Nam, S.B. Oh, B.C. Radburn-Smith, S.h. Seo, U.K. Yang, H.D. Yoo, G.B. Yu

University of Seoul, Seoul, Korea

D. Jeon, H. Kim, J.H. Kim, J.S.H. Lee, I.C. Park

Sungkyunkwan University, Suwon, Korea

Y. Choi, C. Hwang, J. Lee, I. Yu

Vilnius University, Vilnius, Lithuania

V. Dudenas, A. Juodagalvis, J. Vaitkus

National Centre for Particle Physics, Universiti Malaya, Kuala Lumpur, Malaysia

I. Ahmed, Z.A. Ibrahim, M.A.B. Md Ali²⁸, F. Mohamad Idris²⁹, W.A.T. Wan Abdullah, M.N. Yusli, Z. Zolkapli

Centro de Investigacion y de Estudios Avanzados del IPN, Mexico City, Mexico

H. Castilla-Valdez, E. De La Cruz-Burelo, M.C. Duran-Osuna, I. Heredia-De La Cruz³⁰, R. Lopez-Fernandez, J. Mejia Guisao, R.I. Rabadan-Trejo, G. Ramirez-Sanchez, R Reyes-Almanza, A. Sanchez-Hernandez

Universidad Iberoamericana, Mexico City, Mexico

S. Carrillo Moreno, C. Oropeza Barrera, F. Vazquez Valencia

Benemerita Universidad Autonoma de Puebla, Puebla, Mexico

J. Eysermans, I. Pedraza, H.A. Salazar Ibarquen, C. Uribe Estrada

Universidad Autónoma de San Luis Potosí, San Luis Potosí, Mexico

A. Morelos Pineda

University of Auckland, Auckland, New Zealand

D. Krofcheck

University of Canterbury, Christchurch, New Zealand

S. Bheesette, P.H. Butler

National Centre for Physics, Quaid-I-Azam University, Islamabad, Pakistan

A. Ahmad, M. Ahmad, M.I. Asghar, Q. Hassan, H.R. Hoorani, A. Saddique, M.A. Shah, M. Shoaib, M. Waqas

National Centre for Nuclear Research, Swierk, Poland

H. Bialkowska, M. Bluj, B. Boimska, T. Frueboes, M. Górski, M. Kazana, K. Nawrocki, M. Szleper, P. Traczyk, P. Zalewski

Institute of Experimental Physics, Faculty of Physics, University of Warsaw, Warsaw, Poland

K. Bunkowski, A. Byszuk³¹, K. Doroba, A. Kalinowski, M. Konecki, J. Krolikowski, M. Misiura, M. Olszewski, A. Pyskir, M. Walczak

Laboratório de Instrumentação e Física Experimental de Partículas, Lisboa, Portugal

P. Bargassa, C. Beirão Da Cruz E Silva, A. Di Francesco, P. Faccioli, B. Galinhas, M. Gallinaro, J. Hollar, N. Leonardo, L. Lloret Iglesias, M.V. Nemallapudi, J. Seixas, G. Strong, O. Toldaiev, D. Vadrucio, J. Varela

Joint Institute for Nuclear Research, Dubna, Russia

V. Alexakhin, A. Golunov, I. Golutvin, N. Gorbounov, I. Gorbunov, A. Kamenev, V. Karjavin, A. Lanev, A. Malakhov, V. Matveev^{32,33}, P. Moiseenz, V. Palichik, V. Perelygin, M. Savina, S. Shmatov, S. Shulha, N. Skatchkov, V. Smirnov, A. Zarubin

Petersburg Nuclear Physics Institute, Gatchina (St. Petersburg), Russia

V. Golovtsov, Y. Ivanov, V. Kim³⁴, E. Kuznetsova³⁵, P. Levchenko, V. Murzin, V. Oreshkin, I. Smirnov, D. Sosnov, V. Sulimov, L. Uvarov, S. Vavilov, A. Vorobyev

Institute for Nuclear Research, Moscow, Russia

Yu. Andreev, A. Dermenev, S. Gninenko, N. Golubev, A. Karneyeu, M. Kirsanov, N. Krasnikov, A. Pashenkov, D. Tlisov, A. Toropin

Institute for Theoretical and Experimental Physics, Moscow, Russia

V. Epshteyn, V. Gavrilov, N. Lychkovskaya, V. Popov, I. Pozdnyakov, G. Safronov, A. Spiridonov, A. Steppenov, V. Stolin, M. Toms, E. Vlasov, A. Zhokin

Moscow Institute of Physics and Technology, Moscow, Russia

T. Aushev

National Research Nuclear University 'Moscow Engineering Physics Institute' (MEPhI), Moscow, Russia

M. Chadeeva³⁶, P. Parygin, D. Philippov, S. Polikarpov³⁶, E. Popova, V. Rusinov

P.N. Lebedev Physical Institute, Moscow, Russia

V. Andreev, M. Azarkin³³, I. Dremin³³, M. Kirakosyan³³, S.V. Rusakov, A. Terkulov

Skobeltsyn Institute of Nuclear Physics, Lomonosov Moscow State University, Moscow, Russia

A. Baskakov, A. Belyaev, E. Boos, V. Bunichev, M. Dubinin³⁷, L. Dudko, A. Ershov, A. Gribushin, V. Klyukhin, O. Kodolova, I. Lokhtin, I. Miagkov, S. Obraztsov, S. Petrushanko, V. Savrin

Novosibirsk State University (NSU), Novosibirsk, Russia

V. Blinov³⁸, T. Dimova³⁸, L. Kardapoltsev³⁸, D. Shtol³⁸, Y. Skovpen³⁸

State Research Center of Russian Federation, Institute for High Energy Physics of NRC “Kurchatov Institute”, Protvino, Russia

I. Azhgirey, I. Bayshev, S. Bitioukov, D. Elumakhov, A. Godizov, V. Kachanov, A. Kalinin, D. Konstantinov, P. Mandrik, V. Petrov, R. Ryutin, S. Slabospitskii, A. Sobol, S. Troshin, N. Tyurin, A. Uzunian, A. Volkov

National Research Tomsk Polytechnic University, Tomsk, Russia

A. Babaev, S. Baidali

University of Belgrade, Faculty of Physics and Vinca Institute of Nuclear Sciences, Belgrade, Serbia

P. Adzic³⁹, P. Cirkovic, D. Devetak, M. Dordevic, J. Milosevic

Centro de Investigaciones Energéticas Medioambientales y Tecnológicas (CIEMAT), Madrid, Spain

J. Alcaraz Maestre, A. Álvarez Fernández, I. Bachiller, M. Barrio Luna, J.A. Brochero Cifuentes, M. Cerrada, N. Colino, B. De La Cruz, A. Delgado Peris, C. Fernandez Bedoya, J.P. Fernández Ramos, J. Flix, M.C. Fouz, O. Gonzalez Lopez, S. Goy Lopez, J.M. Hernandez, M.I. Josa, D. Moran, A. Pérez-Calero Yzquierdo, J. Puerta Pelayo, I. Redondo, L. Romero, M.S. Soares, A. Triossi

Universidad Autónoma de Madrid, Madrid, Spain

C. Albajar, J.F. de Trocóniz

Universidad de Oviedo, Oviedo, Spain

J. Cuevas, C. Erice, J. Fernandez Menendez, S. Folgueras, I. Gonzalez Caballero, J.R. González Fernández, E. Palencia Cortezon, V. Rodríguez Bouza, S. Sanchez Cruz, P. Vischia, J.M. Vizán García

Instituto de Física de Cantabria (IFCA), CSIC-Universidad de Cantabria, Santander, Spain

I.J. Cabrillo, A. Calderon, B. Chazin Quero, J. Duarte Campderros, M. Fernandez, P.J. Fernández Manteca, A. García Alonso, J. Garcia-Ferrero, G. Gomez, A. Lopez Virto, J. Marco, C. Martinez Rivero, P. Martinez Ruiz del Arbol, F. Matorras, J. Piedra Gomez, C. Prieels, T. Rodrigo, A. Ruiz-Jimeno, L. Scodellaro, N. Trevisani, I. Vila, R. Vilar Cortabitarte

CERN, European Organization for Nuclear Research, Geneva, Switzerland

D. Abbaneo, B. Akgun, E. Auffray, P. Baillon, A.H. Ball, D. Barney, J. Bendavid, M. Bianco, A. Bocci, C. Botta, T. Camporesi, M. Cepeda, G. Cerminara, E. Chapon, Y. Chen, G. Cucciati, D. d’Enterria, A. Dabrowski, V. Daponte, A. David, A. De Roeck, N. Deelen, M. Dobson, T. du Pree, M. Dünser, N. Dupont, A. Elliott-Peisert, P. Everaerts, F. Fallavollita⁴⁰, D. Fasanella, G. Franzoni, J. Fulcher, W. Funk, D. Gigi, A. Gilbert, K. Gill, F. Glege, M. Guilbaud, D. Gulhan, J. Hegeman, V. Innocente, A. Jafari, P. Janot, O. Karacheban¹⁷, J. Kieseler, A. Kornmayer, M. Krammer¹, C. Lange, P. Lecoq, C. Lourenço, L. Malgeri, M. Mannelli, F. Meijers, J.A. Merlin,

S. Mersi, E. Meschi, P. Milenovic⁴¹, F. Moortgat, M. Mulders, J. Ngadiuba, S. Orfanelli, L. Orsini, F. Pantaleo¹⁴, L. Pape, E. Perez, M. Peruzzi, A. Petrilli, G. Petrucciani, A. Pfeiffer, M. Pierini, F.M. Pitters, D. Rabady, A. Racz, T. Reis, G. Rolandi⁴², M. Rovere, H. Sakulin, C. Schäfer, C. Schwick, M. Seidel, M. Selvaggi, A. Sharma, P. Silva, P. Sphicas⁴³, A. Stakia, J. Steggemann, M. Tosi, D. Treille, A. Tsirou, V. Veckalns⁴⁴, W.D. Zeuner

Paul Scherrer Institut, Villigen, Switzerland

L. Caminada⁴⁵, K. Deiters, W. Erdmann, R. Horisberger, Q. Ingram, H.C. Kaestli, D. Kotlinski, U. Langenegger, T. Rohe, S.A. Wiederkehr

ETH Zurich - Institute for Particle Physics and Astrophysics (IPA), Zurich, Switzerland

M. Backhaus, L. Bäni, P. Berger, N. Chernyavskaya, G. Dissertori, M. Dittmar, M. Donegà, C. Dorfer, C. Grab, C. Heidegger, D. Hits, J. Hoss, T. Klijnsma, W. Lustermann, R.A. Manzoni, M. Marionneau, M.T. Meinhard, F. Micheli, P. Musella, F. Nessi-Tedaldi, J. Pata, F. Pauss, G. Perrin, L. Perrozzi, S. Pigazzini, M. Quittnat, D. Ruini, D.A. Sanz Becerra, M. Schönenberger, L. Shchutska, V.R. Tavolaro, K. Theofilatos, M.L. Vesterbacka Olsson, R. Wallny, D.H. Zhu

Universität Zürich, Zurich, Switzerland

T.K. Aarrestad, C. Amsler⁴⁶, D. Brzhechko, M.F. Canelli, A. De Cosa, R. Del Burgo, S. Donato, C. Galloni, T. Hreus, B. Kilminster, I. Neutelings, D. Pinna, G. Rauco, P. Robmann, D. Salerno, K. Schweiger, C. Seitz, Y. Takahashi, A. Zucchetta

National Central University, Chung-Li, Taiwan

Y.H. Chang, K.y. Cheng, T.H. Doan, Sh. Jain, H.R. Jheng, R. Khurana, C.M. Kuo, M.Y. Lee, W. Lin, A. Pozdnyakov, V.L. Quilatan, S.S. Yu

National Taiwan University (NTU), Taipei, Taiwan

P. Chang, Y. Chao, K.F. Chen, P.H. Chen, W.-S. Hou, Arun Kumar, Y.y. Li, R.-S. Lu, E. Paganis, A. Psallidas, A. Steen, J.f. Tsai

Chulalongkorn University, Faculty of Science, Department of Physics, Bangkok, Thailand

B. Asavapibhop, N. Srimanobhas, N. Suwonjandee

Çukurova University, Physics Department, Science and Art Faculty, Adana, Turkey

A. Bat, F. Boran, S. Cerci⁴⁷, S. Damarseckin, Z.S. Demiroglu, F. Dolek, C. Dozen, I. Dumanoglu, S. Girgis, G. Gokbulut, Y. Guler, E. Gurpinar, I. Hos⁴⁸, C. Isik, E.E. Kangal⁴⁹, O. Kara, A. Kayis Topaksu, U. Kiminsu, M. Oglakci, G. Onengut, K. Ozdemir⁵⁰, S. Ozturk⁵¹, D. Sunar Cerci⁴⁷, B. Tali⁴⁷, U.G. Tok, S. Turkcapar, I.S. Zorbakir, C. Zorbilmez

Middle East Technical University, Physics Department, Ankara, Turkey

B. Isildak⁵², G. Karapinar⁵³, M. Yalvac, M. Zeyrek

Bogazici University, Istanbul, Turkey

I.O. Atakisi, E. Gülmez, M. Kaya⁵⁴, O. Kaya⁵⁵, S. Tekten, E.A. Yetkin⁵⁶

Istanbul Technical University, Istanbul, Turkey

M.N. Agarar, S. Atay, A. Cakir, K. Cankocak, Y. Komurcu, S. Sen⁵⁷

Institute for Scintillation Materials of National Academy of Science of Ukraine, Kharkov, Ukraine

B. Grynyov

National Scientific Center, Kharkov Institute of Physics and Technology, Kharkov, Ukraine

L. Levchuk

University of Bristol, Bristol, United Kingdom

F. Ball, L. Beck, J.J. Brooke, D. Burns, E. Clement, D. Cussans, O. Davignon, H. Flacher, J. Goldstein, G.P. Heath, H.F. Heath, L. Kreczko, D.M. Newbold⁵⁸, S. Paramesvaran, B. Penning, T. Sakuma, D. Smith, V.J. Smith, J. Taylor, A. Titterton

Rutherford Appleton Laboratory, Didcot, United Kingdom

K.W. Bell, A. Belyaev⁵⁹, C. Brew, R.M. Brown, D. Cieri, D.J.A. Cockerill, J.A. Coughlan, K. Harder, S. Harper, J. Linacre, E. Olaiya, D. Petyt, C.H. Shepherd-Themistocleous, A. Thea, I.R. Tomalin, T. Williams, W.J. Womersley

Imperial College, London, United Kingdom

G. Auzinger, R. Bainbridge, P. Bloch, J. Borg, S. Breeze, O. Buchmuller, A. Bundock, S. Casasso, D. Colling, L. Corpe, P. Dauncey, G. Davies, M. Della Negra, R. Di Maria, Y. Haddad, G. Hall, G. Iles, T. James, M. Komm, C. Laner, L. Lyons, A.-M. Magnan, S. Malik, A. Martelli, J. Nash⁶⁰, A. Nikitenko⁶, V. Palladino, M. Pesaresi, A. Richards, A. Rose, E. Scott, C. Seez, A. Shtipliyski, G. Singh, M. Stoye, T. Strebler, S. Summers, A. Tapper, K. Uchida, T. Virdee¹⁴, N. Wardle, D. Winterbottom, J. Wright, S.C. Zenz

Brunel University, Uxbridge, United Kingdom

J.E. Cole, P.R. Hobson, A. Khan, P. Kyberd, C.K. Mackay, A. Morton, I.D. Reid, L. Teodorescu, S. Zahid

Baylor University, Waco, USA

K. Call, J. Dittmann, K. Hatakeyama, H. Liu, C. Madrid, B. McMaster, N. Pastika, C. Smith

Catholic University of America, Washington DC, USA

R. Bartek, A. Dominguez

The University of Alabama, Tuscaloosa, USA

A. Buccilli, S.I. Cooper, C. Henderson, P. Rumerio, C. West

Boston University, Boston, USA

D. Arcaro, T. Bose, D. Gastler, D. Rankin, C. Richardson, J. Rohlf, L. Sulak, D. Zou

Brown University, Providence, USA

G. Benelli, X. Coubez, D. Cutts, M. Hadley, J. Hakala, U. Heintz, J.M. Hogan⁶¹, K.H.M. Kwok, E. Laird, G. Landsberg, J. Lee, Z. Mao, M. Narain, J. Pazzini, S. Piperov, S. Sagir⁶², R. Syarif, E. Usai, D. Yu

University of California, Davis, Davis, USA

R. Band, C. Brainerd, R. Breedon, D. Burns, M. Calderon De La Barca Sanchez, M. Chertok, J. Conway, R. Conway, P.T. Cox, R. Erbacher, C. Flores, G. Funk, W. Ko, O. Kukral, R. Lander, C. Mclean, M. Mulhearn, D. Pellett, J. Pilot, S. Shalhout, M. Shi, D. Stolp, D. Taylor, K. Tos, M. Tripathi, Z. Wang, F. Zhang

University of California, Los Angeles, USA

M. Bachtis, C. Bravo, R. Cousins, A. Dasgupta, A. Florent, J. Hauser, M. Ignatenko, N. Mccoll, S. Regnard, D. Saltzberg, C. Schnaible, V. Valuev

University of California, Riverside, Riverside, USA

E. Bouvier, K. Burt, R. Clare, J.W. Gary, S.M.A. Ghiasi Shirazi, G. Hanson, G. Karapostoli, E. Kennedy, F. Lacroix, O.R. Long, M. Olmedo Negrete, M.I. Paneva, W. Si, L. Wang, H. Wei, S. Wimpenny, B.R. Yates

University of California, San Diego, La Jolla, USA

J.G. Branson, S. Cittolin, M. Derdzinski, R. Gerosa, D. Gilbert, B. Hashemi, A. Holzner, D. Klein, G. Kole, V. Krutelyov, J. Letts, M. Masciovecchio, D. Olivito, S. Padhi, M. Pieri, M. Sani, V. Sharma, S. Simon, M. Tadel, A. Vartak, S. Wasserbaech⁶³, J. Wood, F. Würthwein, A. Yagil, G. Zevi Della Porta

University of California, Santa Barbara - Department of Physics, Santa Barbara, USA

N. Amin, R. Bhandari, J. Bradmiller-Feld, C. Campagnari, M. Citron, A. Dishaw, V. Dutta, M. Franco Sevilla, L. Gouskos, R. Heller, J. Incandela, A. Ovcharova, H. Qu, J. Richman, D. Stuart, I. Suarez, S. Wang, J. Yoo

California Institute of Technology, Pasadena, USA

D. Anderson, A. Bornheim, J.M. Lawhorn, H.B. Newman, T.Q. Nguyen, M. Spiropulu, J.R. Vlimant, R. Wilkinson, S. Xie, Z. Zhang, R.Y. Zhu

Carnegie Mellon University, Pittsburgh, USA

M.B. Andrews, T. Ferguson, T. Mudholkar, M. Paulini, M. Sun, I. Vorobiev, M. Weinberg

University of Colorado Boulder, Boulder, USA

J.P. Cumalat, W.T. Ford, F. Jensen, A. Johnson, M. Krohn, S. Leontsinis, E. MacDonald, T. Mulholland, K. Stenson, K.A. Ulmer, S.R. Wagner

Cornell University, Ithaca, USA

J. Alexander, J. Chaves, Y. Cheng, J. Chu, A. Datta, K. Mcdermott, N. Mirman, J.R. Patterson, D. Quach, A. Rinkevicius, A. Ryd, L. Skinnari, L. Soffi, S.M. Tan, Z. Tao, J. Thom, J. Tucker, P. Wittich, M. Zientek

Fermi National Accelerator Laboratory, Batavia, USA

S. Abdullin, M. Albrow, M. Alyari, G. Apollinari, A. Apresyan, A. Apyan, S. Banerjee, L.A.T. Bauerdick, A. Beretvas, J. Berryhill, P.C. Bhat, G. Bolla[†], K. Burkett, J.N. Butler, A. Canepa, G.B. Cerati, H.W.K. Cheung, F. Chlebana, M. Cremonesi, J. Duarte, V.D. Elvira, J. Freeman, Z. Gecse, E. Gottschalk, L. Gray, D. Green, S. Grünendahl, O. Gutsche, J. Hanlon, R.M. Harris, S. Hasegawa, J. Hirschauer, Z. Hu, B. Jayatilaka, S. Jindariani, M. Johnson, U. Joshi, B. Klima, M.J. Kortelainen, B. Kreis, S. Lammel, D. Lincoln, R. Lipton, M. Liu, T. Liu, J. Lykken, K. Maeshima, J.M. Marraffino, D. Mason, P. McBride, P. Merkel, S. Mrenna, S. Nahn, V. O'Dell, K. Pedro, C. Pena, O. Prokofyev, G. Rakness, L. Ristori, A. Savoy-Navarro⁶⁴, B. Schneider, E. Sexton-Kennedy, A. Soha, W.J. Spalding, L. Spiegel, S. Stoynev, J. Strait, N. Strobbe, L. Taylor, S. Tkaczyk, N.V. Tran, L. Uplegger, E.W. Vaandering, C. Vernieri, M. Verzocchi, R. Vidal, M. Wang, H.A. Weber, A. Whitbeck

University of Florida, Gainesville, USA

D. Acosta, P. Avery, P. Bortignon, D. Bourilkov, A. Brinkerhoff, L. Cadamuro, A. Carnes, M. Carver, D. Curry, R.D. Field, S.V. Gleyzer, B.M. Joshi, J. Konigsberg, A. Korytov, P. Ma, K. Matchev, H. Mei, G. Mitselmakher, K. Shi, D. Sperka, J. Wang, S. Wang

Florida International University, Miami, USA

Y.R. Joshi, S. Linn

Florida State University, Tallahassee, USA

A. Ackert, T. Adams, A. Askew, S. Hagopian, V. Hagopian, K.F. Johnson, T. Kolberg, G. Martinez, T. Perry, H. Prosper, A. Saha, A. Santra, V. Sharma, R. Yohay

Florida Institute of Technology, Melbourne, USA

M.M. Baarmand, V. Bhopatkar, S. Colafranceschi, M. Hohlmann, D. Noonan, M. Rahmani, T. Roy, F. Yumiceva

University of Illinois at Chicago (UIC), Chicago, USA

M.R. Adams, L. Apanasevich, D. Berry, R.R. Betts, R. Cavanaugh, X. Chen, S. Dittmer, O. Evdokimov, C.E. Gerber, D.A. Hangal, D.J. Hofman, K. Jung, J. Kamin, C. Mills, I.D. Sandoval Gonzalez, M.B. Tonjes, N. Varelas, H. Wang, X. Wang, Z. Wu, J. Zhang

The University of Iowa, Iowa City, USA

M. Alhusseini, B. Bilki⁶⁵, W. Clarida, K. Dilsiz⁶⁶, S. Durgut, R.P. Gandrajula, M. Haytmyradov, V. Khristenko, J.-P. Merlo, A. Mestvirishvili, A. Moeller, J. Nachtman, H. Ogul⁶⁷, Y. Onel, F. Ozok⁶⁸, A. Penzo, C. Snyder, E. Tiras, J. Wetzel

Johns Hopkins University, Baltimore, USA

B. Blumenfeld, A. Cocoros, N. Eminizer, D. Fehling, L. Feng, A.V. Gritsan, W.T. Hung, P. Maksimovic, J. Roskes, U. Sarica, M. Swartz, M. Xiao, C. You

The University of Kansas, Lawrence, USA

A. Al-bataineh, P. Baringer, A. Bean, S. Boren, J. Bowen, A. Bylinkin, J. Castle, S. Khalil, A. Kropivnitskaya, D. Majumder, W. Mcbrayer, M. Murray, C. Rogan, S. Sanders, E. Schmitz, J.D. Tapia Takaki, Q. Wang

Kansas State University, Manhattan, USA

A. Ivanov, K. Kaadze, D. Kim, Y. Maravin, D.R. Mendis, T. Mitchell, A. Modak, A. Mohammadi, L.K. Saini, N. Skhirtladze

Lawrence Livermore National Laboratory, Livermore, USA

F. Rebassoo, D. Wright

University of Maryland, College Park, USA

A. Baden, O. Baron, A. Belloni, S.C. Eno, Y. Feng, C. Ferraioli, N.J. Hadley, S. Jabeen, G.Y. Jeng, R.G. Kellogg, J. Kunkle, A.C. Mignerey, F. Ricci-Tam, Y.H. Shin, A. Skuja, S.C. Tonwar, K. Wong

Massachusetts Institute of Technology, Cambridge, USA

D. Abercrombie, B. Allen, V. Azzolini, A. Baty, G. Bauer, R. Bi, S. Brandt, W. Busza, I.A. Cali, M. D'Alfonso, Z. Demiragli, G. Gomez Ceballos, M. Goncharov, P. Harris, D. Hsu, M. Hu, Y. Iiyama, G.M. Innocenti, M. Klute, D. Kovalskyi, Y.-J. Lee, P.D. Luckey, B. Maier, A.C. Marini, C. McGinn, C. Mironov, S. Narayanan, X. Niu, C. Paus, C. Roland, G. Roland, G.S.F. Stephans, K. Sumorok, K. Tatar, D. Velicanu, J. Wang, T.W. Wang, B. Wyslouch, S. Zhaozhong

University of Minnesota, Minneapolis, USA

A.C. Benvenuti, R.M. Chatterjee, A. Evans, P. Hansen, S. Kalafut, Y. Kubota, Z. Lesko, J. Mans, S. Nourbakhsh, N. Ruckstuhl, R. Rusack, J. Turkewitz, M.A. Wadud

University of Mississippi, Oxford, USA

J.G. Acosta, S. Oliveros

University of Nebraska-Lincoln, Lincoln, USA

E. Avdeeva, K. Bloom, D.R. Claes, C. Fangmeier, F. Golf, R. Gonzalez Suarez, R. Kamalieddin, I. Kravchenko, J. Monroy, J.E. Siado, G.R. Snow, B. Stieger

State University of New York at Buffalo, Buffalo, USA

A. Godshalk, C. Harrington, I. Iashvili, A. Kharchilava, D. Nguyen, A. Parker, S. Rappoccio, B. Roozbahani

Northeastern University, Boston, USA

G. Alverson, E. Barberis, C. Freer, A. Hortiangtham, D.M. Morse, T. Orimoto, R. Teixeira De Lima, T. Wamorkar, B. Wang, A. Wisecarver, D. Wood

Northwestern University, Evanston, USA

S. Bhattacharya, O. Charaf, K.A. Hahn, N. Mucia, N. Odell, M.H. Schmitt, K. Sung, M. Trovato, M. Velasco

University of Notre Dame, Notre Dame, USA

R. Bucci, N. Dev, M. Hildreth, K. Hurtado Anampa, C. Jessop, D.J. Karmgard, N. Kellams, K. Lannon, W. Li, N. Loukas, N. Marinelli, F. Meng, C. Mueller, Y. Musienko³², M. Planer, A. Reinsvold, R. Ruchti, P. Siddireddy, G. Smith, S. Taroni, M. Wayne, A. Wightman, M. Wolf, A. Woodard

The Ohio State University, Columbus, USA

J. Alimena, L. Antonelli, B. Bylsma, L.S. Durkin, S. Flowers, B. Francis, A. Hart, C. Hill, W. Ji, T.Y. Ling, W. Luo, B.L. Winer, H.W. Wulsin

Princeton University, Princeton, USA

S. Cooperstein, P. Elmer, J. Hardenbrook, P. Hebda, S. Higginbotham, A. Kalogeropoulos, D. Lange, M.T. Lucchini, J. Luo, D. Marlow, K. Mei, I. Ojalvo, J. Olsen, C. Palmer, P. Piroué, J. Salfeld-Nebgen, D. Stickland, C. Tully

University of Puerto Rico, Mayaguez, USA

S. Malik, S. Norberg

Purdue University, West Lafayette, USA

A. Barker, V.E. Barnes, S. Das, L. Gutay, M. Jones, A.W. Jung, A. Khatiwada, B. Mahakud, D.H. Miller, N. Neumeister, C.C. Peng, H. Qiu, J.F. Schulte, J. Sun, F. Wang, R. Xiao, W. Xie

Purdue University Northwest, Hammond, USA

T. Cheng, J. Dolen, N. Parashar

Rice University, Houston, USA

Z. Chen, K.M. Ecklund, S. Freed, F.J.M. Geurts, M. Kilpatrick, W. Li, B. Michlin, B.P. Padley, J. Roberts, J. Rorie, W. Shi, Z. Tu, J. Zabel, A. Zhang

University of Rochester, Rochester, USA

A. Bodek, P. de Barbaro, R. Demina, Y.t. Duh, J.L. Dulemba, C. Fallon, T. Ferbel, M. Galanti, A. Garcia-Bellido, J. Han, O. Hindrichs, A. Khukhunaishvili, K.H. Lo, P. Tan, R. Taus, M. Verzetti

Rutgers, The State University of New Jersey, Piscataway, USA

A. Agapitos, J.P. Chou, Y. Gershtein, T.A. Gómez Espinosa, E. Halkiadakis, M. Heindl, E. Hughes, S. Kaplan, R. Kunnawalkam Elayavalli, S. Kyriacou, A. Lath, R. Montalvo, K. Nash, M. Osherson, H. Saka, S. Salur, S. Schnetzer, D. Sheffield, S. Somalwar, R. Stone, S. Thomas, P. Thomassen, M. Walker

University of Tennessee, Knoxville, USA

A.G. Delannoy, J. Heideman, G. Riley, K. Rose, S. Spanier, K. Thapa

Texas A&M University, College Station, USA

O. Bouhali⁶⁹, A. Castaneda Hernandez⁶⁹, A. Celik, M. Dalchenko, M. De Mattia, A. Delgado, S. Dildick, R. Eusebi, J. Gilmore, T. Huang, T. Kamon⁷⁰, S. Luo, R. Mueller, Y. Pakhotin, R. Patel, A. Perloff, L. Perniè, D. Rathjens, A. Safonov, A. Tatarinov

Texas Tech University, Lubbock, USA

N. Akchurin, J. Damgov, F. De Guio, P.R. Duderov, S. Kunori, K. Lamichhane, S.W. Lee, T. Mengke, S. Muthumuni, T. Peltola, S. Undleeb, I. Volobouev, Z. Wang

Vanderbilt University, Nashville, USA

S. Greene, A. Gurrola, R. Janjam, W. Johns, C. Maguire, A. Melo, H. Ni, K. Padeken, J.D. Ruiz Alvarez, P. Sheldon, S. Tuo, J. Velkovska, M. Verweij, Q. Xu

University of Virginia, Charlottesville, USA

M.W. Arenton, P. Barria, B. Cox, R. Hirosky, M. Joyce, A. Ledovskoy, H. Li, C. Neu, T. Sinthuprasith, Y. Wang, E. Wolfe, F. Xia

Wayne State University, Detroit, USA

R. Harr, P.E. Karchin, N. Poudyal, J. Sturdy, P. Thapa, S. Zaleski

University of Wisconsin - Madison, Madison, WI, USA

M. Brodski, J. Buchanan, C. Caillol, D. Carlsmith, S. Dasu, L. Dodd, S. Duric, B. Gomber, M. Grothe, M. Herndon, A. Hervé, U. Hussain, P. Klabbers, A. Lanaro, A. Levine, K. Long, R. Loveless, T. Ruggles, A. Savin, N. Smith, W.H. Smith, N. Woods

†: Deceased

1: Also at Vienna University of Technology, Vienna, Austria

2: Also at IRFU, CEA, Université Paris-Saclay, Gif-sur-Yvette, France

3: Also at Universidade Estadual de Campinas, Campinas, Brazil

4: Also at Federal University of Rio Grande do Sul, Porto Alegre, Brazil

5: Also at Université Libre de Bruxelles, Bruxelles, Belgium

6: Also at Institute for Theoretical and Experimental Physics, Moscow, Russia

7: Also at Joint Institute for Nuclear Research, Dubna, Russia

8: Also at Cairo University, Cairo, Egypt

9: Also at Helwan University, Cairo, Egypt

10: Now at Zewail City of Science and Technology, Zewail, Egypt

11: Also at Department of Physics, King Abdulaziz University, Jeddah, Saudi Arabia

12: Also at Université de Haute Alsace, Mulhouse, France

13: Also at Skobeltsyn Institute of Nuclear Physics, Lomonosov Moscow State University, Moscow, Russia

14: Also at CERN, European Organization for Nuclear Research, Geneva, Switzerland

15: Also at RWTH Aachen University, III. Physikalisches Institut A, Aachen, Germany

16: Also at University of Hamburg, Hamburg, Germany

17: Also at Brandenburg University of Technology, Cottbus, Germany

18: Also at MTA-ELTE Lendület CMS Particle and Nuclear Physics Group, Eötvös Loránd University, Budapest, Hungary

19: Also at Institute of Nuclear Research ATOMKI, Debrecen, Hungary

20: Also at Institute of Physics, University of Debrecen, Debrecen, Hungary

21: Also at Indian Institute of Technology Bhubaneswar, Bhubaneswar, India

22: Also at Institute of Physics, Bhubaneswar, India

23: Also at Shoolini University, Solan, India

24: Also at University of Visva-Bharati, Santiniketan, India

25: Also at Isfahan University of Technology, Isfahan, Iran

26: Also at Plasma Physics Research Center, Science and Research Branch, Islamic Azad University, Tehran, Iran

27: Also at Università degli Studi di Siena, Siena, Italy

28: Also at International Islamic University of Malaysia, Kuala Lumpur, Malaysia

- 29: Also at Malaysian Nuclear Agency, MOSTI, Kajang, Malaysia
- 30: Also at Consejo Nacional de Ciencia y Tecnología, Mexico city, Mexico
- 31: Also at Warsaw University of Technology, Institute of Electronic Systems, Warsaw, Poland
- 32: Also at Institute for Nuclear Research, Moscow, Russia
- 33: Now at National Research Nuclear University 'Moscow Engineering Physics Institute' (MEPhI), Moscow, Russia
- 34: Also at St. Petersburg State Polytechnical University, St. Petersburg, Russia
- 35: Also at University of Florida, Gainesville, USA
- 36: Also at P.N. Lebedev Physical Institute, Moscow, Russia
- 37: Also at California Institute of Technology, Pasadena, USA
- 38: Also at Budker Institute of Nuclear Physics, Novosibirsk, Russia
- 39: Also at Faculty of Physics, University of Belgrade, Belgrade, Serbia
- 40: Also at INFN Sezione di Pavia ^a, Università di Pavia ^b, Pavia, Italy
- 41: Also at University of Belgrade, Faculty of Physics and Vinca Institute of Nuclear Sciences, Belgrade, Serbia
- 42: Also at Scuola Normale e Sezione dell'INFN, Pisa, Italy
- 43: Also at National and Kapodistrian University of Athens, Athens, Greece
- 44: Also at Riga Technical University, Riga, Latvia
- 45: Also at Universität Zürich, Zurich, Switzerland
- 46: Also at Stefan Meyer Institute for Subatomic Physics (SMI), Vienna, Austria
- 47: Also at Adiyaman University, Adiyaman, Turkey
- 48: Also at Istanbul Aydin University, Istanbul, Turkey
- 49: Also at Mersin University, Mersin, Turkey
- 50: Also at Piri Reis University, Istanbul, Turkey
- 51: Also at Gaziosmanpasa University, Tokat, Turkey
- 52: Also at Ozyegin University, Istanbul, Turkey
- 53: Also at Izmir Institute of Technology, Izmir, Turkey
- 54: Also at Marmara University, Istanbul, Turkey
- 55: Also at Kafkas University, Kars, Turkey
- 56: Also at Istanbul Bilgi University, Istanbul, Turkey
- 57: Also at Hacettepe University, Ankara, Turkey
- 58: Also at Rutherford Appleton Laboratory, Didcot, United Kingdom
- 59: Also at School of Physics and Astronomy, University of Southampton, Southampton, United Kingdom
- 60: Also at Monash University, Faculty of Science, Clayton, Australia
- 61: Also at Bethel University, St. Paul, USA
- 62: Also at Karamanoğlu Mehmetbey University, Karaman, Turkey
- 63: Also at Utah Valley University, Orem, USA
- 64: Also at Purdue University, West Lafayette, USA
- 65: Also at Beykent University, Istanbul, Turkey
- 66: Also at Bingol University, Bingol, Turkey
- 67: Also at Sinop University, Sinop, Turkey
- 68: Also at Mimar Sinan University, Istanbul, Istanbul, Turkey
- 69: Also at Texas A&M University at Qatar, Doha, Qatar
- 70: Also at Kyungpook National University, Daegu, Korea